Zr^{IV}-tetraphenylporphyrinates as Nuclease Mimics: Structural, Kinetic and Mechanistic Studies on Phosphate Diester Transesterification

Eugen Stulz,[a] Hans-Beat Bürgi,[b] and Christian Leumann*[a]

Abstract: The Zr^{IV}-tetraphenylporphyrinates Zr(TPP)(X,X′), (X,X′ = $^-$OAc, $^-$OMe, Cl^-) **4**–**6**, **8** were prepared and their complexing properties as well as catalytic properties towards solvolysis of the phosphate diesters hpp (**2**), dmp (**3**) and pmp (**16**) characterised. The diesters **2** and **16**, representing model phosphates for RNA and DNA, were substrates for the catalyst $Zr(TPP)Cl_2$ (**4**), and rate accelerations over background by 6–9 orders of magnitude were measured. These accelerations are comparable to those of dinuclear transition metal catalysts and lanthanide ions. Catalytic turnover was observed. Kinetic studies revealed that the catalytically active species of **4** in the solvolysis of **2** and **16** in methanol-containing solvents are dinuclear complexes containing either one or two phosphate esters depending upon the phosphate concentration. Besides the usual solvolysis pathway of the RNA model hpp (**2**), which proceeds via the cyclophosphate **20**, a second, unusual pathway via direct substitution of the hydroxypropyl substituent was found. X-ray analysis of the Zr(TPP)(dmp) complex **19** revealed a dinuclear structure with two bridging dmp ligands and one monomethyl phosphate unit. In **19** one of the two dmp residues occurs in a very unusual high energy *ac*,*ap* conformation. Based on this structure and on the kinetic data, mechanistic models for the two solvolysis reaction pathways were developed. From an extensive CSD search on phosphodiester structures no correlation between P–O ester bond lengths and diester conformations could be found. However, P–O ester bonds decrease in length with increasing formal charge of the complexing metal ions. This underlines the higher importance of electrostatic activation relative to stereoelectronic effects in phosphodiester hydrolysis.

Keywords: bioinorganic chemistry · catalysts · phosphatases · porphyrinoids · zirconium

Introduction

The design and synthesis of molecules that function as artificial nucleases has become a field of great interest in the past decade. Such compounds may lead to powerful new drugs acting at the level of gene expression, or to new tools in biotechnology.[1] Most compounds investigated so far are transition metal complexes,[2] lanthanide complexes[3] or small molecules with basic functional groups[4] that may be attached to nucleic acid recognising units for sequence specific RNA or DNA cleavage.[5]

In natural nucleases, two major pathways for activating and cleaving the phosphate diester group can be differentiated: i) hydrolysis is induced either by a general acid–base mechanism where His, Lys or Glu usually determine the catalytic cascade (e.g. RNAse A,[6] RNAse T1[7]); or ii) the negative charge of the phosphate diester group is neutralised by a metal ion (electrostatic activation), and a metal-bound water or hydroxide serves as the nucleophile (e.g. DNAse I,[8] pyrophosphatase[9]). The most active enzymes combine the two features in their active site, such as staphylococcal nuclease (Ca^{2+}, Arg)[10] or nuclease S1 (Zn^{2+}, Lys).[11] The power of such a combination is exemplified by staphylococcal nuclease,[12] which accelerates the hydrolysis of DNA by a factor of 10^{16}, relative to background. The contribution attributed to the metal ion is estimated to be about $10^{4.6}$.[13] This reduces the calculated lifetime of DNA from million years to milliseconds.[14]

The reactivity of simple metal complexes can thus be substantially increased by attachment of basic or nucleophilic side chains to the ligand system. In this way rate enhancements arise from either an additional complexation of the basic side chain to the phosphate diester, stabilising the pentacovalent intermediate phosphorane,[1a,15] or from deprotonation of a metal-bound water.[16]

In our search for structures that could serve as building blocks for artificial nucleases, combining Lewis acid activation

[a] Prof. Dr. C. Leumann, E. Stulz
Department of Chemistry and Biochemistry
University of Bern
Freiestrasse 3, 3012 Bern (Switzerland)
Fax: (+41) 31-631-3422
E-mail: leumann@ioc.unibe.ch

[b] Prof. Dr. H.-B. Bürgi
Laboratory of Chemical and Mineralogical Crystallography
University of Bern
Freiestrasse 3, 3012 Bern (Switzerland)

  0947-6539/00/0603-0523 $ 17.50+.50/0

and general acid–base catalysis, we identified Zr^{IV}-tetraphenylporphyrinates ($[Zr^{IV}(TPP)]^{2+}$) as ideal candidates. Zirconium porphyrinates are robust (class II) complexes[17] that can only be demetallated under strongly acidic conditions such as sulphuric acid or HF. Therefore, they can be regarded as virtually inert towards demetallation under physiological conditions.[18] Porphyrins have a rigid and planar geometry, and are easy to synthesise in a variety of different substitution patterns. Zr^{IV}-porphyrinates show "out-of-plane" geometries[19] with additional ligands always in *cis* position relative to the porphyrin plane.

For 60 years Zr^{4+}-salts have been known to exhibit "phosphatatic activity".[20] But only recently has Zr^{IV} been rediscovered for this purpose.[21] We have shown that the complex $Zr^{IV}(acac)_2(sae)$ (**1**) (sae = *N*-2-hydroxyethylsalicylideneiminato) promotes the solvolysis of 2-hydroxypropyl phenyl phosphate (hpp) (**2**) with a rate acceleration of about 10^9 (benzene/methanol 1:1), obeying Michaelis–Menten kinetics.[22] Here we report on the use of Zr^{IV}-tetraphenylporphyrin complexes in phosphate diester transesterification. In particular we investigated i) the influence of different ligands and of different solvents on the complexation of dimethyl phosphate (dmp) **3** with Zr(TPP)(X,X′) (X,X′ = $^-$OAc, $^-$OMe or Cl^-); ii) the crystal structure of a Zr(TPP)-dmp complex; and iii) the mechanistic and kinetic properties of $Zr(TPP)Cl_2$ (**4**) induced solvolysis of phosphate diesters **2** and **16** under various conditions.

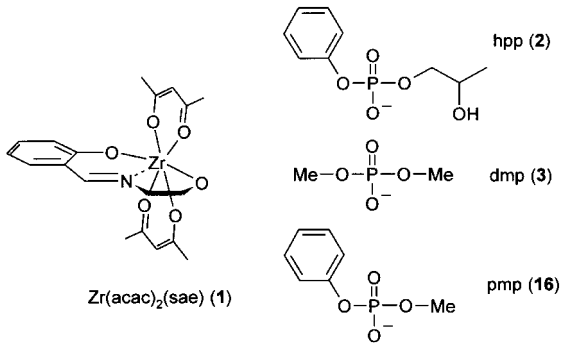

Results and Discussion

Synthesis of Zr(TPP)(X,X′): Zirconium porphyrinates were synthesised mainly according to adapted literature procedures. The insertion of zirconium into $H_2(TPP)$ was achieved by a method analogous to that of Buchler.[23] $Zr(TPP)(OAc)_2$ (**5**) was obtained in an overall yield of 93% (Scheme 1).[24]

Zr(TPP)(OAc,Cl) (**6**) and $Zr(TPP)Cl_2$ (**4**) were prepared from $Zr(TPP)(OAc)_2$ (**5**) analogous to the corresponding octaethylporphyrin (OEP)-derivatives reported by Brand and Arnold[25] with $SiCl_4$ (**5**→**4**) or Me_3SiCl (**5**→**6**) in refluxing anhydrous toluene. The yields were 90% for $Zr(TPP)Cl_2$ (**4**) and 91% for Zr(TPP)(OAc,Cl) (**6**). While compound **4** is already known,[26] compound **6** has not been reported so far.

Attempts to prepare the derivatives $Zr(TPP)(OMe)_2$ (**7**) and Zr(TPP)(OAc,OMe) (**8**) were only partially successful.

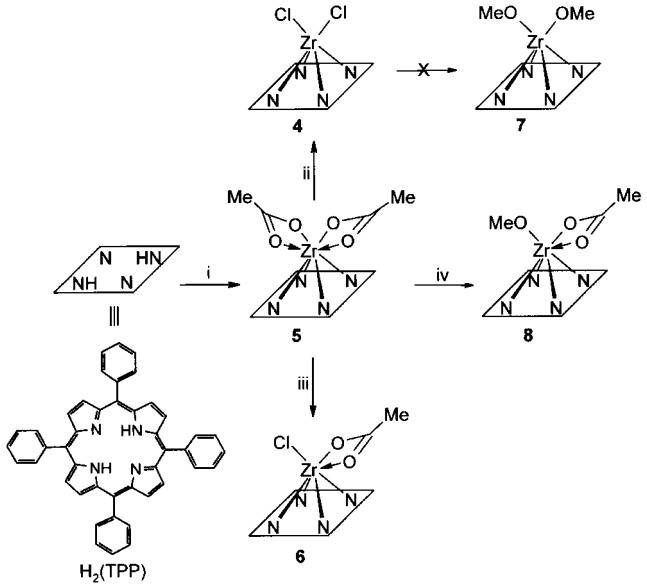

Scheme 1. i) a) $Zr(acac)_4$, phenol, 1,2,4-trichlorobenzene, 240 °C, 24 h, b) pyridine/HOAc, reflux, 2 h, then H_2O, 93%; ii) $SiCl_4$, toluene, reflux, 7 h, 90%; iii) Me_3SiCl, toluene, reflux, 7 h, 91%; iv) a) Me_3SiCl, toluene, reflux, 3 h, b) KOMe/MeOH, 80 °C (3 h) →RT, 12 h, ca. 96%.

We were unable to prepare **7** from **4** with KOMe or NaOMe in toluene, methanol or mixtures thereof. Compound **8** could not be obtained analytically pure, although the in situ transformation of Zr(TPP)(OAc,Cl) (**6**) with KOMe/methanol yielded ligand exchange from chloride to methoxide to an extent of 90–95% (^{1}H-NMR spectral evidence). The failure to prepare Zr-porphyrinate–methoxide complexes was also reported by Brand and Arnold for the corresponding octaethylporphyrin derivatives.[25]

Zirconium porphyrinates **4**–**6** and **8** are well soluble in chlorinated solvents, toluene, benzene and pyridine with a characteristic blood-red colour, but virtually insoluble in methanol and water. In mixtures of chloroform or benzene with methanol or methanol/water and in DMSO/chloroform solutions (with or without water) the zirconium porphyrinates can be dissolved to a maximum concentration of ca. 10 mM. Addition of bases such as imidazole or triethylamine reduces the solubility in chloroform/methanol to about 1 mM and gives rapid and complete precipitation from water containing solvents.

Complex formation properties of Zr(TPP)(X,X′) towards phosphate diesters: In order to test the ability of zirconium porphyrinates to bind phosphate diesters we performed complexation experiments with hpp (**2**) and dmp (**3**) using $Zr(TPP)Cl_2$ (**4**), $Zr(TPP)(OAc)_2$ (**5**), Zr(TPP)(OAc,Cl) (**6**) and Zr(TPP)(OAc,OMe) (**8**). For solubility reasons the experiments were done in $CDCl_3/CD_3OD$, C_6D_6/MeOH, $[D_6]$DMSO/$CDCl_3$ and $[D_6]$DMSO/$CDCl_3/H_2O$ solvent mixtures and were examined by ^{1}H/^{31}P-NMR spectroscopy.

In a first set of experiments we mixed **4**, **5**, **6** and **8** separately with dmp (**3**) in $CDCl_3/CD_3OD$ 9:1 (Table 1). The NMR spectra showed new signals for dmp (**3**) at δ=1.51 in the ^{1}H-NMR and at $\delta = -18$ in the ^{31}P-NMR spectrum (free dmp: $\delta = 3.58$ and $\delta = 3$ in the ^{1}H-NMR and ^{31}P-NMR spectrum,

0947-6539/00/0603-0524 $ 17.50+.50/0 *Chem. Eur. J.* **2000**, *6*, No. 3

Table 1. Complexation of dmp (**3**) various Zr(TPP)-complexes in $CDCl_3$/CD_3OD 9:1.

Zr porphyrinate[a]	Zr(TPP):dmp (**3**) ratio[b]	total ligand exchange [%]
$Zr(TPP)(OAc)_2$ (**5**)	1:2.5	0
Zr(TPP)(OAc)Cl (**6**)	1:2.9	20
Zr(TPP)(OAc)OMe (**8**)	1:1.3	17
$Zr(TPP)Cl_2$ (**4**)	1:1	50
$Zr(TPP)Cl_2$ (**4**)	1:2	82
$Zr(TPP)Cl_2$ (**4**)	1:2.6	89

[a] [**5**] = 7.5 mM, [**6**] = 8.1 mM, [**8**] = 7.9 mM, [**4**] = 8.6 mM. [b] Exact ratio determined by ^{1}H-NMR.

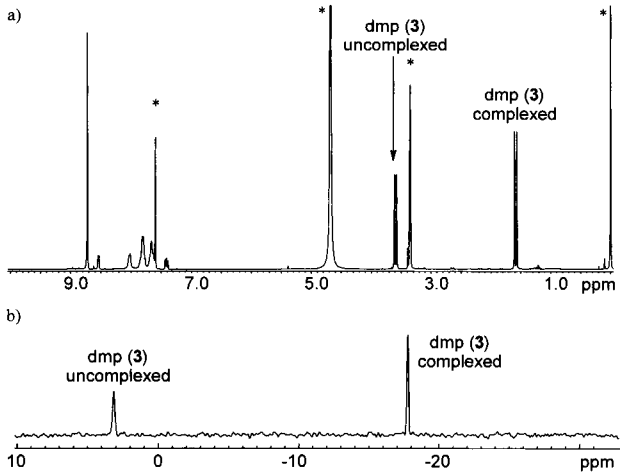

Figure 1. a) ^{1}H-NMR (300 MHz) and b) ^{31}P-NMR spectrum (81 MHz) of the mixture of dmp (**3**) with $Zr(TPP)Cl_2$ (**4**) in $CDCl_3$/CD_3OD after four days. In a) residual proton signals of solvent and internal reference (TMS, $\delta = 0$) are marked with an asterisk.

respectively). The ligand exchange reactions were essentially complete after 5 min. Figure 1 displays a representative NMR experiment. All signals were sharp lines, indicating strong binding and slow exchange between free and complexed phosphate on the NMR time scale.[27] The observed high-field shifts for complexed dmp (**3**) relative to free dmp (**3**) were $\Delta\delta = \sim 2$ ppm (^{1}H NMR) and of $\Delta\delta = \sim 20$ ppm (^{31}P NMR). This is consistent with a general upfield shift of ligands complexed to metal porphyrinates due to the ring current of the aromatic porphyrin ligand system.[28]

During the complexation with dmp (**3**) only methoxide and chloride ligands exchanged, but not acetate (Table 1). The general trend in the relative rate and amount of exchange is acetate $\ll$ methoxide $<$ chloride. The inertness of acetate as ligand on $[Zr(TPP)]^{2+}$ towards ligand exchange with dmp(**3**) can only be explained by a chelate effect, because compared with the pK_a values of the corresponding acids (HCl -7, HOAc 4.7, MeOH 15.5) acetate should be exchanged considerably faster than methoxide. We assume that complexes of the stoichiometry Zr(TPP)(OAc,dmp) (**13**), Zr(TPP)(Cl,dmp) (**14**) and $Zr(TPP)(dmp)_2$ (**15**) were formed (Scheme 2).

We note that complexes **14** and **15** cannot be distinguished by NMR spectroscopy. For the methyl protons of dmp (**3**) complexed to $[Zr(TPP)]^{2+}$ always only one signal (doublet, $J_{P-H} = 11$ Hz) was observed. This indicates complexation of dmp (**3**) in a monodentate way. The second ligand on

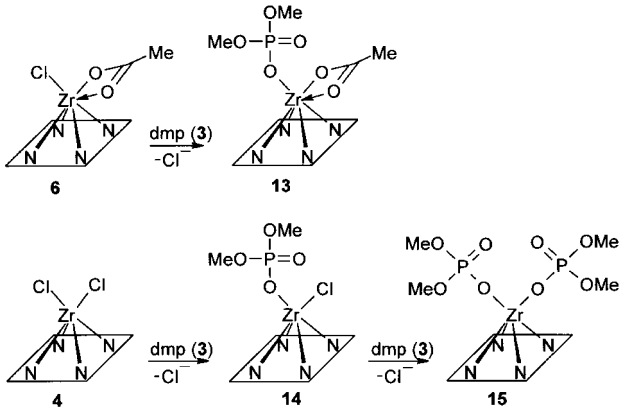

Scheme 2. Complexation of **4** and **6** with dmp (**3**).

Zr(TPP)(dmp,X) (X = Cl^- or dmp) seems to have no effect on the chemical shift of the complexed phosphate. In the ^{1}H-NMR spectrum of **13** the resonances assigned to complexed dmp (**3**) ($\delta = 1.58$) are slightly shifted ($\Delta\delta = 0.14$ ppm) towards lower field compared with the dmp-signals in **14** or **15** ($\delta = 1.44$).

A second set of experiments was performed to determine the relative rates of ligand exchange from chloride to phosphate. An approximately 10 mM solution of Zr(TPP)-(OAc,Cl) (**6**) or $Zr(TPP)Cl_2$ (**4**) was mixed with dmp (**3**) (1:1 and 1:2, respectively) in $CDCl_3$/CD_3OD 5:2 (Table 2).

Table 2. Second order rate constants for the ligand exchange reactions **4** → **14** and **6** → **13** (see Scheme 2) in $CDCl_3$/CD_3OD 5:2.

Zr-porphyrinate[a]	Zr(TPP):dmp ratio	k_2 [$M^{-1}s^{-1}$]
$Zr(TPP)Cl_2$ (**4**)	1:2	0.13
Zr(TPP)(OAc)Cl (**6**)	1:1	3.6×10^{-3}

[a] [**4**] = 10.7 mM, [**6**] = 11.4 mM.

The increased methanol concentration in the solvent mixture allowed the reaction to be followed by ^{1}H-NMR spectroscopy. With Zr(TPP)(OAc,Cl) (**6**) a pure second order reaction to produce **13** was anticipated (Scheme 2). The rate constant was calculated using Equation (1) (see Experimental Section). In the case of $Zr(TPP)Cl_2$ (**4**) we calculated a relative second order rate constant from the initial rate v_0 of ligand exchange on $Zr(TPP)Cl_2$ (**4**) according to Equation (2) (Experimental Section) assuming that the rate limiting step is bimolecular (although the true rate constant for the overall reaction is of higher order). The initial rate v_0 (2.93×10^{-5} M s^{-1}) was determined from the slope of the exponential fit to the measured concentration of free dmp (**3**) versus time at $t = 0$ (Figure 2).

The relative rate for the ligand exchange on $Zr(TPP)Cl_2$ (**4**) is about 36 times faster than for Zr(TPP)(OAc)Cl (**6**) (Table 2). Complex **4** showed 55% exchange after 30 min and 65% after five days, in **6** ligand exchange reached saturation after two days (83%). This saturation effect is most probably due to methanol being a competitor to phosphate as a ligand.

We also performed complexation experiments with the RNA model hpp (**2**) using $Zr(TPP)Cl_2$ (**4**), $Zr(TPP)(OAc)_2$

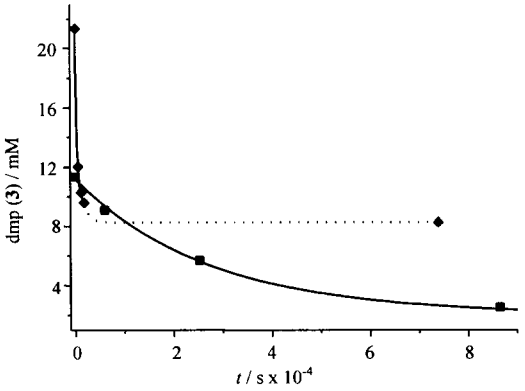

Figure 2. Time dependent concentration of free dmp (**3**), observed by ^{1}H-NMR spectroscopy, for the complexation of dmp (**3**) with ◆ Zr(TPP)Cl_2 (**4**) and ■ Zr(TPP)(OAc)Cl (**6**) in $CDCl_3/CD_3OD$ 5:2. Solid curves are fitted exponential curves. The dotted line corresponds to an extrapolation.

(**5**) and Zr(TPP)(OAc,Cl) (**6**) (stoichiometric ratio of Zr:P = 1:3 in each mixture) that were followed by ^{31}P-NMR spectroscopy. Due to solubility reasons the solvent was changed to [D_6]DMSO/$CDCl_3$ 5:2. Complexes **5** and **6** showed no affinity to hpp (**2**) in this solvent. The dichloride **4**, however, complexed hpp (**2**) rapidly (< 3 min) under formation of two new species with sharp signals at $\delta = -16$ and $\delta = -18$ (free hpp (**2**): $\delta = -5$) with a 1:1 Zr:hpp stoichiometry (Figure 3a).

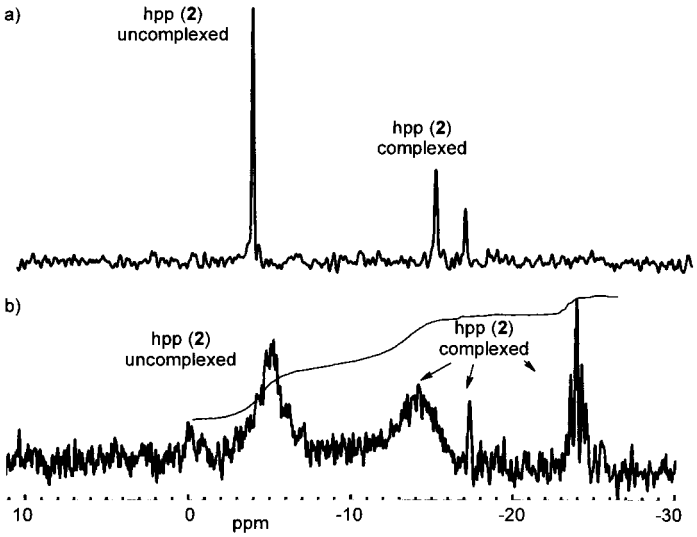

Figure 3. ^{31}P-NMR spectra (81 MHz) of Zr(TPP)Cl_2 (**4**) in the presence of hpp (**2**): a) in [D_6]DMSO/$CDCl_3$ 5:2; and b) in [D_6]DMSO/$CDCl_3/H_2O$ 10:5:1.

Integration indicates that 41 % of hpp (**2**) is uncomplexed and 59 % refer to a 1:1 Zr:hpp complex. This leads to an apparent dissociation constant K_a of 800 M^{-1}.

Addition of H_2O ([D_6]DMSO/$CDCl_3/H_2O$ 10:5:1) led to significant broadening of two signals ($\delta = -5$ and -18), and a new set of sharp signals arose at $\delta = -24$ (Figure 3b). This spectrum remained unchanged over a period of two weeks, and extraction experiments with water/acetic acid yielded only hpp (**2**) and the diacetato-complex **5** as determined by UV/Vis, HPLC and ^{1}H/^{31}P-NMR spectroscopy. No products as a result of hydrolysis of hpp (**2**) were identified. The line broadening indicates a dynamic exchange process between bound and free species. Therefore complexation of hpp (**2**) may be reversible in the presence of water, and the phosphate can be quantitatively displaced from zirconium porphyrinates by acetic acid. The observation that under aqueous conditions upfield shifts of the complexed phosphate of as much as $\Delta\delta =$ 20 ppm appear is in agreement with the formation of dinuclear complexes. For such species a doubled ring current effect induced by two porphyrin units is expected (vide infra).

Similar experiments were performed with Zr(TPP)Cl_2 (**4**) and dmp (**3**) in C_6D_6/MeOH (1:1). This system was chosen in view of the solvolysis experiments to be described later.

From the ^{31}P-NMR spectra it is obvious that in this solvent mixture the complexation with dmp (**3**) is concentration dependent. The line broadening of the signals referring to complexed and free dmp (**3**) (Figure 4) are reminiscent for slow exchange processes.

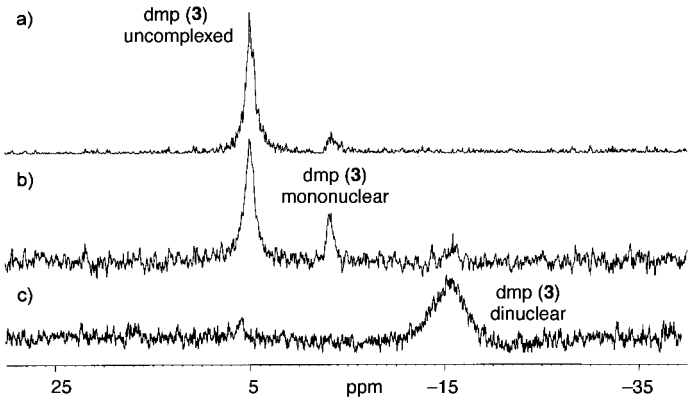

Figure 4. ^{31}P-NMR spectra (121 MHz) of Zr(TPP)Cl_2 (**4**) in the presence of dmp (**3**) in C_6D_6/MeOH 1:1; a) Zr:P = 1:8, b) Zr:P = 1:2.5, c) Zr:P = 1:0.1.

A variety of Zr(TPP)(dmp) complexes with chemical shifts at $\delta = -3$ and at $\delta = -16$ are formed depending on the relative zirconium and phosphate concentrations. We attribute the signal at $\delta = -3$ to mononuclear and the signal at $\delta = -16$ to dinuclear complexes in accordance with the ring current effect of the porphyrins.

Apparent dissociation constants (K_d) for the Zr(TPP)-(dmp) complexes were determined from these ligand exchange reactions (Table 3). Assuming that with an excess of phosphate over zirconium porphyrinate (8:1) only complexes with the composition Zr(TPP)$(dmp)_2$ **15** are formed, a K_d of 45.3 mM was calculated. This value compares well with that determined for the distinct 1:1 complex of dmp (**3**) with **1** (K_d 76.2 mM).[22] If an excess of zirconium porphyrinate over phosphate (1:0.1) is used, the formation of (μ-dmp)[Zr-(TPP)]$_2$(X)$_3$ (**17**) (Scheme 3) should be favoured, and a K_d of 0.61 mM results. With intermediate stoichiometries of phosphate to zirconium a mixture of **14**, **15**, **17** and **18** is produced and the apparent K_d of 1.51 mM agrees with that determined for the complexation of hpp (**2**) by Zr(TPP)Cl_2 (**4**) in [D_6]DMSO/$CDCl_3/H_2O$ 10:5:1 (K_d = 1.25 mM).

The complexation of dmp (**3**) in a dinuclear complex is 75 times stronger compared with a mononuclear species. This is

0947-6539/00/0603-0526 $ 17.50+.50/0 *Chem. Eur. J.* **2000**, *6*, No. 3

Table 3. Dissociation constants calculated from the ligand exchange reactions of **4** and **1** with dmp (**3**) and hpp (**2**) in various solvent mixtures and phosphate/zirconium (Zr:P) ratios

Zr complex	phosphate diester	solvent Zr/P ratio	K_d [mM]
$Zr(TPP)Cl_2$ (**4**)	dmp (**3**)	in C_6D_6/MeOH 1:1	
		1:8	45.3
		1:2.5	1.51
		1:0.1	0.61
	hpp (**2**)	in $[D_6]$DMSO/$CDCl_3$/H_2O 10:5:1	1.25
$Zr(acac)_2(sae)$ (**1**)	dmp (**3**)	in C_6D_6/MeOH 1:1	76.2[22]
		1:4	

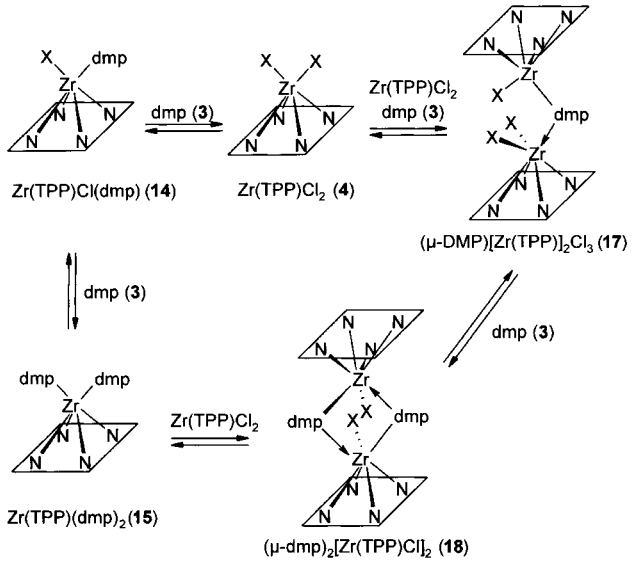

Scheme 3. Complex formation equilibria between $Zr(TPP)Cl_2$ (**4**) and dmp (**3**) in solution. Further structures are not excluded. X = Cl^-, MeO^-.

in accordance with the observed difference in phosphate complexation with mononuclear and dinuclear cobalt(III) complexes.[29] In contrast to the complexation of phosphates with $Zr(acac)_2(sae)$ (**1**),[22] $Zr(TPP)Cl_2$ (**4**) complexes dmp (**3**) about 1.6 times stronger than a mononuclear and about 125 times stronger than a dinuclear complex. Two reasons might be responsible for this: i) **1** has only one complexation site for phosphates, whereas **4** contains potentially four such sites, ii) addition of a phosphate diester to **1** leads to a charged complex whereas exchange of Cl anion by such an ester in **4** leaves the product complex neutral.

In summary the results of the complexation experiments indicate that: i) complexes with different zirconium/phosphate stoichiometry exist in solution (Scheme 3); ii) the nature of the preferred complex and its stability with respect to the NMR time scale strongly depends on the solvent, the zirconium/phosphate ratio and the investigated zirconium porphyrinate itself; iii) dmp (**3**) is complexed most likely in a monodentate way; iv) hpp (**2**) presumably forms a chelate between the phosphate and the alkoxide group.

Crystal structure of (μ-η^2-mmp)(μ-dmp)$_2$[ZrTPP]$_2$ (19): Isolation of a crystalline zirconium-porphyrinate-phosphate ester complex from $Zr(TPP)Cl_2$ (**4**) or Zr(TPP)(OAc)Cl (**6**) with either hpp (**2**) or dmp (**3**) proved to be difficult. A mixture of a toluene solution of **4** or **6** with a methanol solution of **2** or **3** yielded only sparingly soluble, powdery products. From $CDCl_3$/methanol, however, a dmp-complex of **4** could be isolated and single crystals suitable for X-ray analysis could be grown in an anhydrous toluene/pentane mixture at $-20\,^\circ C$ within one and a half month. The structure of the complex (Figure 5) was determined to be (μ-η^2-mmp)-(μ-dmp)$_2$[Zr(TPP)]$_2$ (**19**) (as a bis-toluene solvate; mmp = monomethyl phosphate) and represents the first crystal structure of a Zr^{IV}-porphyrinate-phosphate complex.

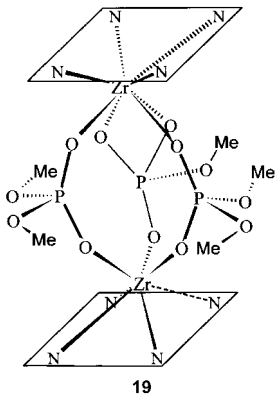

In this compound two μ-dmp units and one μ-η^2-monomethyl phosphate (mmp) bridge two zirconium ions and form a "sandwich" complex, reminiscent of the complexes of hydroxo- and oxo-bridged zirconium porphyrinates.[30] All terminal oxygen atoms of phosphates are complexed. The occurrence of a monomethyl phosphate in the structure can only be explained assuming diffusion of water into the solution during crystallisation and subsequent hydrolysis of dmp (**3**).

The phosphate part of the crystal structure is highly disordered with an apparent inversion centre midway between the two zirconium atoms. Figures 5 and 6 show one of the two symmetry equivalent arrangements of the phosphate esters. Although the pocket formed by the two Zr(TPP) entities has approximate C_4 symmetry, only two arrangements of the phosphate esters could be detected (related by the apparent inversion centre). The methyl group of the monomethyl phosphate shows additional disorder and was assigned to two equally populated but different positions. The structure refinement was restrained to show equal P–O(ester)-,

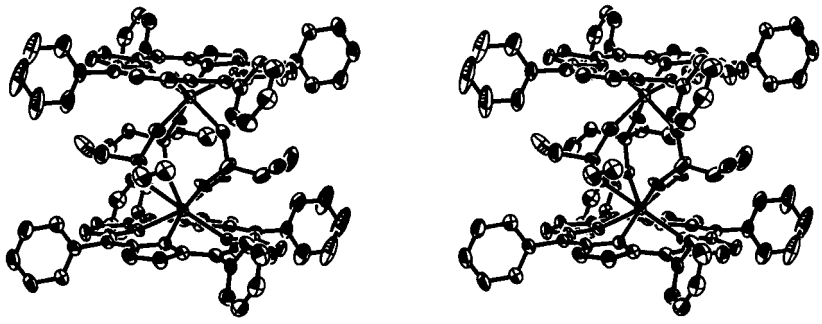

Figure 5. Stereoplot of (μ-η^2-mmp)(μ-dmp)$_2$[Zr(TPP)]$_2$ (**19**) (50% probability level). Only one of the two equivalent orientations of the phosphate esters is shown (see text). Hydrogen atoms are omitted for clarity.

P–O(Zr)- and C–O(P)-bond lengths, respectively. Releasing these restraints resulted in esd′s which were much larger than the differences between individual bond lengths.

The coordination polyhedra around the two zirconium ions are different for a given arrangement of the phosphates. One zirconium shows a 4+3-type polyhedron with a square-planar base formed by the four nitrogens of the porphyrin, and a trigonal planar cap formed by three phosphate oxygens; the second zirconium exhibits a square-antiprismatic coordination geometry with the four nitrogen and four oxygen atoms forming squares. In Figure 6 a top view perpendicular to the porphyrin planes of the coordination sphere around the zirconium atom is drawn.

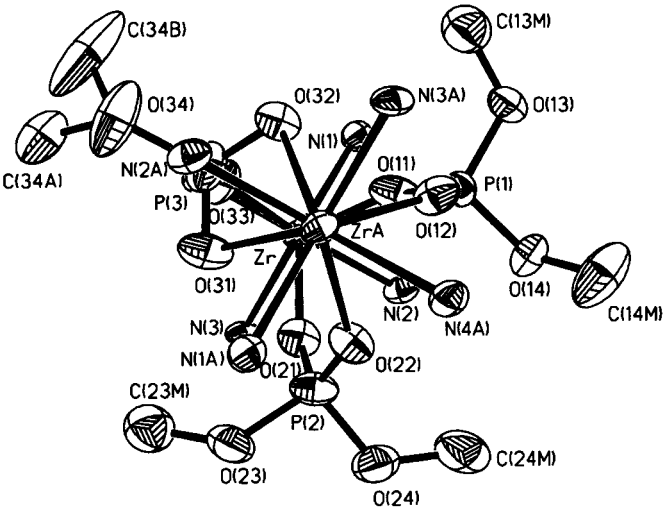

Figure 6. Top-view of the coordination sphere around the Zr atoms in **19** and numbering scheme for one of the two equally probable orientations of the phosphates (50% probability level, H-Atoms omitted). C(34A, B) highlight the disordered methyl groups of the μ,η^2-mmp ligand.

In the analoguous complexes $\{(\mu\text{-OH})_3[Zr(TPP)]_2\}(7,8\text{-}C_2B_9H_{12})$ and $(\mu\text{-O})(\mu\text{-}(OH)_2)]Zr(TPP)]_2$ the geometry around zirconium is also found to be of the 4+3-type,[30a] whereas in $(\mu\text{-OH})_4[Zr(TPP)]_2$ the zirconium coordination is square-antiprismatic.[30b] The complex **19** seems to be the first with mixed geometries of the two zirconium ions. The Zr–N bond lengths range from 2.285(6) to 2.303(5) Å (average 2.295(9)) and represent values in the upper range found in zirconium porphyrinates so far (range 2.222(1) to 2.293(1) Å).[25,26,30,31] The Zr–O bond lengths are in the range of 2.071(9) to 2.244(15) Å (average 2.181(7)). The Zr atom is displaced 1.1 Å from the N_4 plane; these values do not represent extrema.[30] The two porphyrinates are eclipsed: the torsion angles N1-Zr-ZrA-N3A and N2-Zr-ZrA-N4A are 3.3° and −3.0°, respectively. The same conformation has been found in the oxo- and hydroxo-bridged Zr(TPP) complexes.[30] The distance between the two Zr atoms is 5.07 Å, which is significantly longer than the metal–metal distance found in dinuclear phosphodiesterases (3–4 Å).[29] Additionally, two Zr–N bonds and two bonds of the phosphate monoester (P3–O33 and P3–O34) are coplanar with torsion angles being N4-Zr-O33-P3 180(2)°, N2-Zr-O33-P3 −13(3)° and Zr-O33-P3-O34 −176(1)°.

An interesting structural feature is the conformation of the phosphate diesters. The torsion angles C-O-P-O (Table 4) in the phosphate P1 are in the *sc*,*ap* (*gauche*,*trans*) range, and those in the phosphate P2 adopt an almost ideally stretched −*ac*,*ap* conformation.

Table 4. Torsion angles of the phosphate diesters in $(\mu\text{-}\eta^2\text{-mmp})(\mu\text{-dmp})_2[Zr(TPP)]_2$ (**19**).

parameter	deg (esd)	parameter	deg (esd)
O14-P1-O13-C13M	−178(4)	O24-P2-O23-C23M	−134(3)
O13-P1-O14-C14M	76(2)	O23-P2-O24-C24M	−166(2)

These geometries do not correspond to the preferred *sc*,*sc* (or −*sc*,−*sc*) range usually found in aliphatic, noncyclic phosphate diesters;[32] especially the −*ac*,*ap* conformation is very unusual. There is no simple explanation, that is in terms of steric constraints, for this observation. The *trans* conformation lacks stabilization via the anomeric effect. The calculated increase in total energy is 5.4 kJ mol^{-1} for the *sc*,*ap* and 15.1 kJ mol^{-1} for the −*ac*,*ap* conformation, relative to the most stable *sc*,*sc* conformation of free dmp (**3**).[33] Torsion angles in the *ap* range have been reported only in crystals containing uncharged phosphates (triesters, protonated diesters) or aryl substituted phosphate diesters; the existence of the *ap*,*ap* conformer was also postulated in solution for dmp (**3**) on the basis of ^{31}P-NMR spectroscopy.[34]

Phosphate geometry: The observed, very unusual phosphate conformation of dmp (**3**) in the structure of **19** prompted us to perform a search of the Cambridge Structural Database (CSD), similar to that performed by Schneider et al.[33] The search was restricted to aliphatic (C_{sp3}), noncyclic phosphate diesters of charge −1 (including metal complexes) and an *R* factor of ⩽6% (error-free refinements); 22 entries were found (mainly dinucleotides, dimethyl phosphates, diethyl phosphates and dibutyl phosphates) with 31 different geometries for which a two dimensional diagram of the torsion angles O_{ester}-P-O-C was plotted (Figure 7).

Because the CSD programs assign the torsion angles T1 and T2 to the two P–O-ester bonds in a random way, and because either one or the other of two enantiomers is stored in the CSD, the values of T1 and T2 were exchanged and their signs changed to obtain all four isoenergetic structures of a general diester conformation. The diagram (overall *cmm* symmetry) clearly shows that the distribution of the torsion angles has its highest density in the *sc*,*sc* and −*sc*,−*sc* range (22 structures), and a scattered distribution along a "circle line" centred at 180°,180° with a radius of 120°. Some density is found in the *sc*,*ap* range (6 structures). This pattern is similar to the calculated energy diagram for dmp (**3**).[32] Contrary to the *sc*,*ap* conformation the *ap*,−*ac* conformation of dmp (**3**) in **19** has no precedence in the CSD and therefore represents a unique geometry for dmp (**3**) in a crystal.

Surprisingly, the analysis of these diesters showed that the conformation of the phosphate group has no obvious effect on the different P–O bond lengths, and no *gauche* effect could be detected in the bond parameters. This observation is consistent with the calculated P–O(ester) bond lengths for dmp (**3**)

0947-6539/00/0603-0528 $ 17.50+.50/0 *Chem. Eur. J.* **2000**, *6*, No. 3

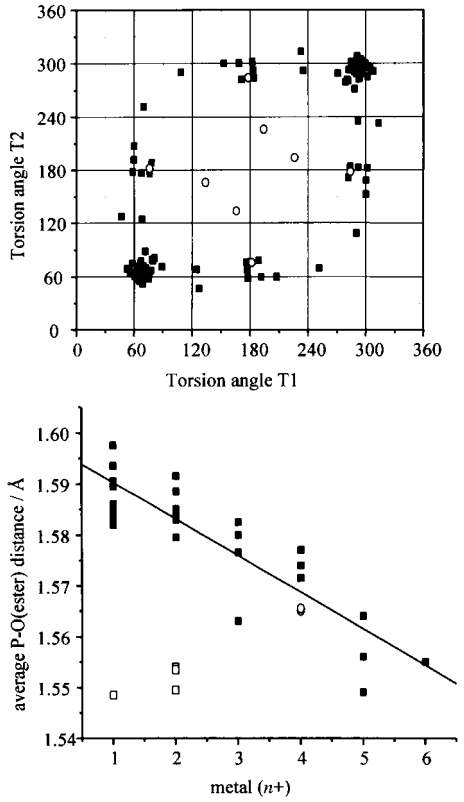

Figure 7. Top: scatter diagram of torsion angles T1 and T2 for phosphate diesters; bottom: plot of average P–O(ester) bond lengths against formal charge of the counterion (linear correlation is $d = 1.597 - 0.0072n^+$, $r = 0.880$). ■ structures from CSD-search (search-profile and □ outlayers from linear correlation see text), ○ values of (μ-η^2-mmp)(μ-dmp)$_2$[ZrTPP]$_2$ **19**.

in the gas phase,[35] where the bond lengths are shortened by only 0.003 Å on going from a *sc*,*sc* to an *ap*,*ap* conformation. The average bond lengths obtained from our search (P–O(ester) 1.576(2) Å, P=O 1.486(2) Å)[36] are comparable to those determined by Schneider et al.[33] (1.595(15) Å and 1.485(13) Å)), and to the average bond lenghts in **19** (P–O(ester) 1.564(4) Å and P=O 1.489(3) Å). It has been noted that the sum of the P–O bond lengths is a constant parameter for phosphates. Values of 6.184 Å[37] and 6.160 Å[33] have been reported. Our search yielded a value of 6.125 Å. The sums of the bond lengths in **19** are slightly lower than these average values (6.108 Å).

Although the phosphate ester bond lengths in the crystal structures of our CSD search appears to be independent of conformation, two trends can still be discerned: i) a lengthening of one P–O(ester) bond tends to be associated with a lengthening of the other P–O(ester) bond, and ii) a lengthening of the average P–O(ester) bond tends to be associated with a slight shortening of the average P=O bond. A finding which is perhaps more significant concerns a linear dependence of the average P–O(ester) bond length on the formal charge of the metal counterion (Figure 7; for monovalent organic cations as counterions to the phosphate diester a charge of +1 was taken).

The bond length contracts by about 0.05 Å on going from a M(+1) to a M(+6) complex. The complex **19** fits well in this line, too. The position of the counterion relative to the charged oxygen atom of the phosphate group and the nuclearity of the phosphate complex also had a slight influence on the P–O(ester) bond, especially among the M(+2) class, where most examples were available. Here the average bond length is shortened by about 0.01 Å per direct counterion contact. Two structures are clearly out of the linear correlation: one is polymeric Ag^+(η-diethyl phosphate)[38] (one crystallographically independent PO_4-group) and the other is a catena-Zn^{2+}(η-dmp)[39] structure (four independent PO_4-groups). The silver diethyl phosphate complex showed moderate to large thermal motion (or disorder), which results in rather uncertain bond length parameters. For the catena-Zn^{2+}(η-dmp) complex no explanation for the short P–O(ester) bond lengths can be given. We found no significant correlations of counterion charge (and position) with any other geometrical parameter, except that P=O bond lengths tend to increase with increasing oxidation number of the counterion, as expected from the negative correlation between the P–O(ester) and the P=O bond lengths.

Metals in a high oxidation state are generally hard and strong Lewis acids.[40] Hence complexation with the hard phosphate anion increases the positive partial charge on the phosphorus and with this its electrophilicity. This is reflected in short P–O(ester) bonds (Figure 7). Schneider et al.[33] determined the average P–O(ester) bond lengths as a function of the charge on the phosphate. Here a clear shortening of the ester bond length (1.621 Å, 1.595 Å and 1.563 Å, respectively) was found with decreasing charge of the phosphate group from −2 to 0. The average P–O(ester) bond lengths of the metal complexes found in the CSD are between the values calculated for phosphate triesters and phosphate diesters.

An alternative way to evaluate the relative amount of positive charge and therefore the electrophilicity on phosphorus is ^{31}P-NMR spectroscopy. Unfortunately, we could not find data in the literature which are comparable with respect to nature of the phosphate diester, counterions, solvents and chemical shift reference, that would allow a comparison of the phosphorus chemical shift versus type of counterion. Such an investigation still awaits realisation.

Stereoelectronic effects have been invoked in discussions on phosphate ester hydrolysis.[41] To explain their significant influence on the calculated total energy of the phosphate diester as well as of the pentacovalent phosphorane intermediate, the role of lone pairs has been discussed from both a theoretical and an experimental point of view.[42] The suggestions are that phosphate diesters with *sc*,*ac* or *sc*,*ap* conformations are more labile and are therefore more rapidly hydrolysed than phosphate diesters in a *sc*,*sc* conformation. The data presented in this paper show that lone pair interactions do not lead to significant changes of P–O(ester) bond lengths and may therefore be assumed not to contribute significantly to a weakening of the corresponding bond. The evidence given above does suggest, however, that the bond lengths in phosphate diesters are shortened, and the electrophilicity of the phosphorous atom thus increased, by increasing electrostatic effects.

Such Lewis acid activation is also supported by the observed rates of hydrolysis of phosphate esters (triester >

diester > monoester[44]) which perfectly correlate with the trend in the corresponding bond lengths. Furthermore, the available kinetic data show that higher-valent metal ions[45] (e. g. Ce^{3+} vs. Ce^{4+})[46] are more efficient promotors for phosphate diester hydrolysis than lower valent metal ions. This is consistent with more recent ab initio calculations on phosphate ester hydrolysis[43] which showed that the rate determining step is the nucleophilic attack on the phosphorus. Taken together, the evidence given here suggests that activation of phosphate esters towards hydrolysis is mainly achieved by Lewis acid activation, and that nuclease mimics combining several highly charged metal ions in the active species should perform particularly well.

Kinetics and mechanisms of transesterification of phosphate diesters with Zr(TPP)Cl_2 (4): Transesterification experiments were performed in anhydrous as well as in water-containing solvents. Due to solubility reasons C_6D_6/methanol 1:1, C_6D_6/methanol/H_2O 5:5:1, [D_6]DMSO/$CHCl_3$/H_2O 5:5:1 and $CHCl_3$/methanol 1:1 were chosen as reaction media. The phosphate substrates were hpp (**2**) (RNA model) and pmp (**16**) (DNA model). The progress of the transesterification reactions were followed by ^{31}P-NMR spectroscopy or UV/Vis spectroscopy. All reactions were performed by using the Zr(TPP)Cl_2 (**4**) in substoichiometric amounts.

In a first set of experiments with hpp (**2**) as substrate, we performed Michaelis–Menten kinetics with variable concentration of hpp (**2**) ([**2**] = 8 to 40 mM) and constant concentration of Zr(TPP)Cl_2 (**4**) ([**4**] = 2 mM) in C_6D_6/methanol 1:1 (T = 28 °C). In order to get insight into the overall reaction order, we also varied the concentrations of Zr(TPP)Cl_2 (**4**) ([**4**] = 1 to 5 mM at [**2**] = 32 mM). The progress of the transesterification of hpp (**2**) was monitored by ^{31}P-NMR spectroscopy, and all reactions were followed to completion. Since intermediates could also be identified and quantified, the reactions were treated as consecutive irreversible pseudo first order reactions **A** → **B** → **C**. The corresponding rate constants k_1 (first step **A** → **B**) and k_1' (second step **B** → **C**) were obtained by curve fitting to the measured concentrations of the phosphates.[47] Figure 8 gives representative examples.

The variation of zirconium or phosphate concentrations, which were undertaken to determine the individual reaction orders, presented an unexpected picture of the reactivity of Zr(TPP)Cl_2 (**4**) towards hpp (**2**) (Scheme 4).

Analysis of the solvolysis products with ^{31}P-NMR spectroscopy and MALDI-TOF-MS revealed that at low Zr/P ratios (< 1:14) the solvolysis reaction proceeded via the cyclic phosphate **20** as an intermediate to produce the methyl hydroxypropyl phosphates **21**. This product distribution is in agreement with pathway a) in Scheme 4. It is analogous to the hydrolysis pathway of RNA and its model phosphates. At high Zr/P ratios (> 1:4), however, pmp (**16**) and dmp (**3**) appeared as products (Scheme 4, pathway b). No traces of the cyclic phosphate **20** could be observed under these conditions. In this pathway, the first step must include substitution of propanediol by methanol, followed by methanolysis to dmp (**3**) with phenol as leaving group. Intermediate stoichiometries of Zr:P resulted in superposition of the two reaction

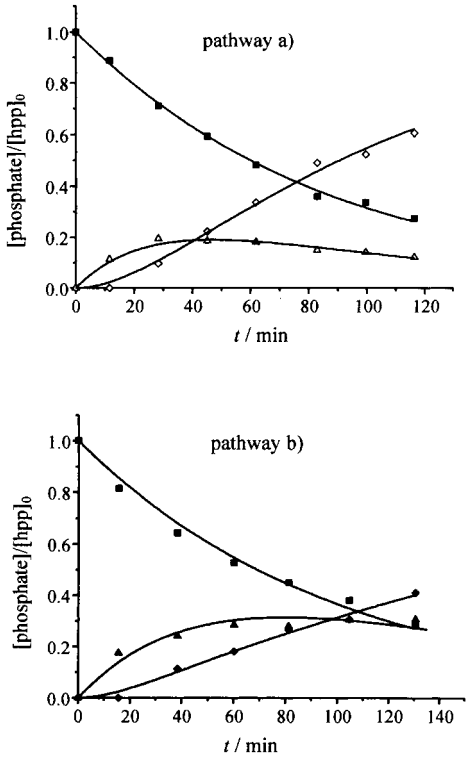

Figure 8. Time dependence of the concentrations of phosphates relative to hpp (**2**), C_6D_6/methanol 1:1, T = 28 °C. Top: according to pathway a) (Scheme 4): ■ hpp (**2**), △ **20**, ◇ **21** ([**4**] = 2 mM, [**2**] = 32 mM); bottom: according to pathway b) (Scheme 4): ■ hpp (**2**), ▲ pmp (**16**), ◆ dmp (**3**) ([**4**] = 2 mM, [**2**] = 8 mM). Solid lines are fitted according to the equations used for a consecutive irreversible first order reaction.[47]

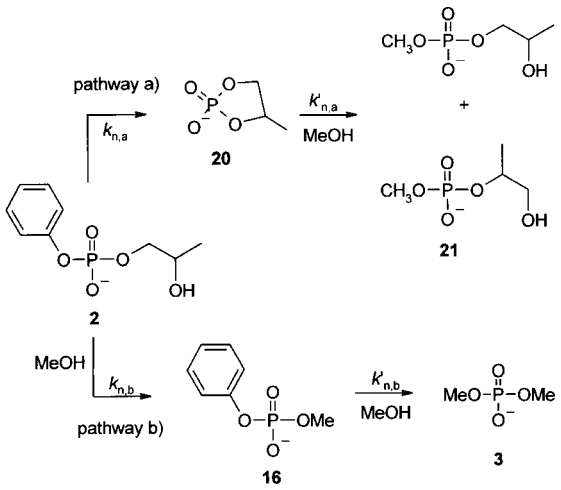

Scheme 4. The two reaction pathways observed for the transesterification of hpp (**2**) as a function of the Zr:phopshate ratio.

pathways. Obviously, hpp (**2**) can be transesterifed with Zr(TPP)Cl_2 (**4**) via at least two different reaction channels. The pathway b) for hydrolysis of α-hydroxy phosphates is very unusual and has not been reported so far.

The reaction is second order in **4** at all concentrations investigated (Figure 9, top), indicating double Lewis acid activation of the solvolysis. This is consistent with the dissociation constants determined by direct measurement with dmp (**3**), and especially with the crystal structure of **19**,

0947-6539/00/0603-0530 $ 17.50+.50/0 *Chem. Eur. J.* **2000**, *6*, No. 3

strongly suggesting it to be a catalytically active complex. The reaction order in phosphate changed continuously from first order at high zirconium/phosphate ratios (>1:4) to second order at lower Zr/P ratios (<1:14) (Figure 9, bottom). Parallel

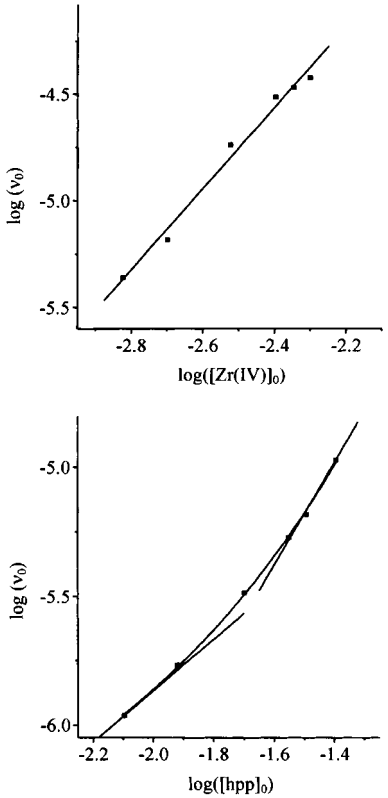

Figure 9. Double logarithmic plot of initial rates versus concentration of **4** (top) or **2** (bottom) for determination of the reaction orders in the solvolysis of **2** with **4** (C_6D_6/methanol 1:1, $T=28\,^{\circ}C$). Slope of the linear regression for **4** is 1.89 ($r=0.994$). For **2** the curve is an exponential fit with tangents having slopes of 1 and 2, respectively.

to this change in reaction order the pathway according to which hpp (**2**) was transesterified changed from pathway b) to pathway a) (Scheme 4). The overall order of the "usual" reaction according to pathway a) is therefore four with an active species of the stoichiometry $[Zr(TPP)]_2(hpp)_2(OMe)_x$, whereas the overall order of the reaction according to pathway b) is three and involves a complex of the type $[Zr(TPP)]_2(hpp)(OMe)_x$. For the unusual pathway b) we propose a mechanistic model of hydrolysis, in which hpp (**2**) forms a chelate complex with a zirconium porphyrinate (Figure 10, left). This prevents the hydroxyl group of the side chain from acting as an intramolecular nucleophile. Instead, the active nucleophile is methanol, which could be activated by hydrogen bonding to alcoholates complexed to Zr. In contrast, the 2:2 Zr:P complex may have only bridging monodentate phosphates (in accordance with the structure of **19**) leading to the "normal" hydrolytic pathway a) for hpp (**2**) (Figure 10, right).

Analysis of the kinetic parameters according to Michaelis–Menten was no longer possible because the initial reaction rate (at constant concentration of **4**) increased with increasing concentration of phosphate, which can be explained by the

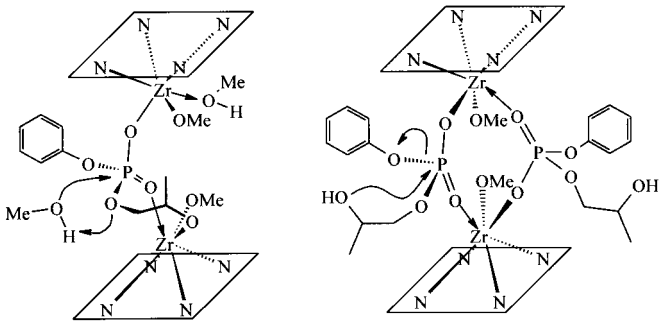

Figure 10. Models proposed for the active complex in the third order reaction leading to solvolysis of hpp (**2**) according to pathway b) in Scheme 4 (left) and in the fourth order reaction resulting in the usually observed transesterification of hpp (**2**) (right).

superposition of the two different reaction mechanisms. The pseudo first order rate constants observed for variable Zr concentrations (at constant phosphate concentration) showed a linear dependence on the zirconium concentration for both k_1 (**2**→**20**) and k_1' (**20**→**21**). In these experiments only solvolysis according to pathway a) (Scheme 4) was observed. Apparent second order rate constants k_2 and k_2' are needed to quantify acceleration and have been obtained from the slopes of the corresponding linear regressions (Table 5) regardless of the overall higher reaction orders.

Table 5. Apparent first and second order rate constants and relative rate accelerations for the solvolysis of hpp (**2**) with $Zr(TPP)Cl_2$ (**4**) (C_6D_6/methanol 1:1, $T=28\,^{\circ}C$).

	k_2 [$M^{-1}s^{-1}$]	k_{cat} [s^{-1}] [a]	k_{rel} [b]
hpp (**2**) → **20**	0.31[c]	1.6×10^{-4}	8.7×10^{6}
20 → **21**	0.50[c]	2.5×10^{-4}	20×10^{6}
hpp (**2**) → pmp (**16**)	0.09[d]	0.45×10^{-4}	–
pmp (**16**) → dmp (**3**)	0.12[d]	0.6×10^{-4}	3062×10^{6}

[a] $k_{cat}=k_2\times K_d$.[48] [b] $k_{rel}=k_{cat}/k_{1,0}$ where $k_{1,0}$ is the first order rate constant for the background reaction (**2**→**20**: $1.85\times10^{-11}\,s^{-1}$, **20**→**21**: $1.24\times10^{-11}\,s^{-1}$, **16**→**3**: $1.96\times10^{-14}\,s^{-1}$).[49] [c] From linear correlations of k_1 vs. $[Zr]_0$. [d] From single measurement.[50]

Assuming an average dissociation constant of $K_d\sim0.5$ mM for the complexation of the phosphates in a dinuclear complex,[48] an apparent k_{cat} for the reactivity of the supramolecular zirconium-phosphate complex can be estimated and compared with the background reaction.[49] The rate accelerations determined this way are in the range of 9×10^6 to 3.1×10^9, and are comparable to those observed for Th^{IV} salts[51] and for dinuclear Co^{III} complexes.[2e] The production of **16** from **2** cannot be compared with a background reaction since this reaction did not take place without **4**, neither under basic or acidic, nor under thermal conditions. It is surprising, indeed, that the acceleration of the methanolysis of pmp (**16**) is about 350 times larger than that of the transesterification of the more labile RNA-model hpp (**2**).

To investigate the influence of a general base we performed a transesterification experiment with addition of excess imidazole, in which hpp (**2**) or pmp (**16**) were used as substrate. In $CHCl_3$/methanol 1:4 ($T=30\,^{\circ}C$) the concentrations of the phosphates were varied in the range of 0.25 to 4.0 mM at constant concentration of $Zr(TPP)Cl_2$ (**4**) ([**4**]=

1 mM, [imidazole] = 20 mM). The progress of the reactions had to be followed by UV/Vis spectroscopy because of the low phosphate concentrations and the generally fast reactions (virtually complete after ~4 h). The substrate hpp (**2**) produced only **21**, and pmp (**16**) was transesterified to dmp (**3**) according to analysis by ^{31}P-NMR spectroscopy.

Determination of the initial rates of the reactions revealed that for both phosphates saturation kinetics could be observed with turnover number ~1.3 (Figure 11). The inhibitor proved

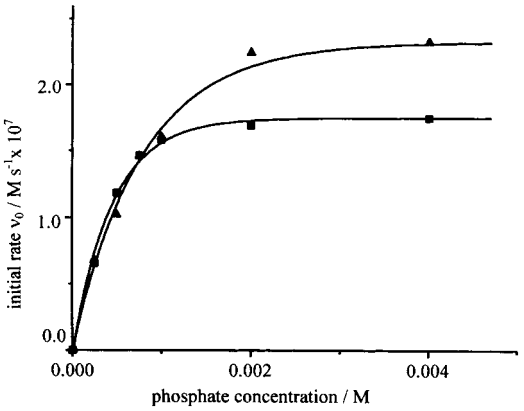

Figure 11. Saturation kinetics of the transesterification of ■ hpp (**2**) and ▲ pmp (**16**) with Zr(TPP)Cl$_2$ (**4**) in CHCl$_3$/methanol 1:4 ([**4**] = 1 mM, [imidazole] = 20 mM, T = 30 °C) including sigmoidal curve fits.

to be the released phenol, because in the presence of a large excess of phenol under otherwise identical conditions no transesterification took place. Evaluation of the kinetic parameters according to the usual equations used for saturation kinetics[47] yielded k_{cat} and K_M (Table 6).

Table 6. Kinetic parameters and relative rate enhancements for the transesterification of phosphate diesters with **4** obeing saturation kinetics (CHCl$_3$/methanol 1:4, [**4**] = 1 mM, [imidazole] = 20 mM, [**2**] = 0.25 to 4.0 mM, T = 30 °C).

Phosphate diester	k_{cat} [s^{-1}]	K_M [mM]	k_2[a] [M^{-1}s^{-1}]	k_{rel}[b]
hpp (**2**)	1.75×10^{-4}	0.44	0.40	6.93×10^3
pmp (**16**)	2.32×10^{-4}	0.79	0.29	28.5×10^3

[a] $k_2 = k_{cat}/K_M$. [b] $k_{rel} = k_2/k_{2,0}$, where $k_{2,0}$ is the second order rate constant for the imidazole induced background reaction (for **2**: 5.74×10^{-5} M^{-1}s^{-1}, for **16**: 1.03×10^{-5} M^{-1}s^{-1}).

Inspection of the values shows that hpp (**2**) is bound to Zr(TPP)Cl$_2$ (**4**) almost twice as strongly as pmp (**16**). This stronger binding of hpp (**2**) to **4** may be due in part to the hydroxypropyl side chain in **2** which provides one important structural difference to **16**. The magnitude of the dissociation constants K_M of the supramolecular zirconium phosphate complexes indicates the presence of a dinuclear species which is also the catalytically active molecule in the hydrolytic step for both phosphates **2** and **16**.

The rate acceleration for the solvolysis of the more robust DNA model pmp (**16**) is about four times larger than for the labile RNA model hpp (**2**). The fact that **16** is depleated faster than **2** indicates that not only an intramolecular attack of an alcohol (or alcoholate) is of significance, but a nucleophile from the solvent (either free or metal bound) is central in the rate determining step. The intramolecular nucleophile, the hydroxyl group of the side chain, is deactivated upon complexation. The relative rate accelerations are about three orders of magnitude lower than for the solvolysis in the absence of imidazole (in C$_6$D$_6$/methanol, see above). It is not clear at this point, why imidazole decreases the reaction rates.

Finally the solvolysis experiments were also performed in water containing solvents. Under mildly acidic conditions (buffered solution C$_6$D$_6$/methanol/H$_2$O 5:5:1, 100 mM imidazole/HCl pH 6.0)[52] solvolysis of hpp (**2**) took place, but precipitation of Zr^{IV}-porphyrinates occured during the experiments. This lead to decreasing velocity of the reaction which terminated after ~57% turnover (turnover number 4.6, Figure 12).

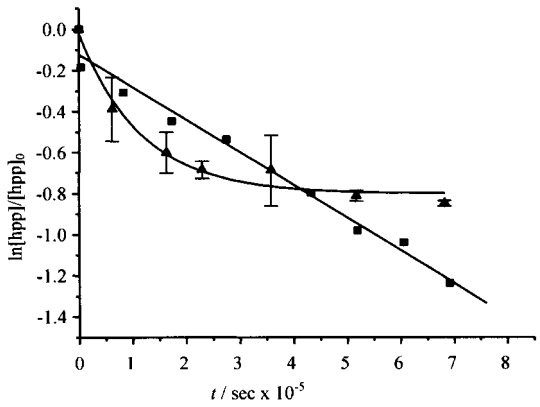

Figure 12. Decay rates of hpp (**2**) in the presence of Zr(TPP)Cl$_2$ (**4**); ▲ in C$_6$D$_6$/MeOH/H$_2$O 5:5:1 ([**4**] = 1.5 mM, [**2**] = 12 mM, 100 mM imidazole/HCl pH 6.0) with exponential curve fit, ■ in [D$_6$]DMSO/CHCl$_3$/H$_2$O 5:5:1 ([**4**] = 8 mM, [**2**] = 24 mM, [H$^+$] = 40 mM) with pseudo first order linear regression (r = 0.993).

The initial rate ($v_0 = 7.4 \times 10^{-8}$ M s^{-1}) of the reaction, however, allowed the calculation of an apparent k_1 for the first stage of the reaction by using Equation (3) (Table 7). From this, an acceleration of 3.7×10^6 relative to the calculated background rate[53] is determined. This increase in reactivity is comparable to the rate enhancements determined in anhydrous C$_6$D$_6$/methanol 1:1, although this is true only for the first stage of the transesterification reaction. The product distribution indicated the occurrence of both pathways a) and b) (Scheme 4) for this experiment.

Hydrolytic activity of Zr(TPP)Cl$_2$ (**4**) towards hpp (**2**) in its protonated form (H-hpp **H-2**) in otherwise unbuffered

Table 7. Pseudo first order rate constants for the solvolysis of hpp (**2**) with Zr(TPP)Cl$_2$ (**4**) in water-containing solvents (T = 40 °C) with relative rate enhancements.

Solvent	Zr:Phosphate ratio	k_1 [s^{-1}]	$k_1/k_{1,0}$
C$_6$D$_6$/MeOH/H$_2$O 5:5:1 (imidazole/HCl pH 6.0)[a]	1:8	5.02×10^{-5}	3.72×10^6
[D$_6$]DMSO/CHCl$_3$/H$_2$O 5:5:1 (40 mM H$^+$)[b]	1:3	$1.59 \pm 0.084 \times 10^{-6}$	4.95

[a] [**4**] = 1.5 mM, [**2**] = 12 mM, buffer 100 mM. [b] [**4**] = 8 mM, [**H-2**] = 24 mM, [H$^+$] = 40 mM[54]; for $k_{1,0}$ see [59].

0947-6539/00/0603-0532 $ 17.50+.50/0 *Chem. Eur. J.* **2000**, *6*, No. 3

solution ([D_6]DMSO/$CHCl_3$/H_2O 5:5:1, $T = 40\,^{\circ}C$) was measured by following the solvolysis reaction with ^{31}P-NMR spectroscopy (Figure 12). In this experiment no precipitation occurred. Analysis of the kinetic data according to the usual procedure for pseudo first order reactions [Eq. (4)] revealed that the relative rate acceleration dropped to ~ 5 over background (Table 7). This relatively low acceleration is due to the large rate of the autosolvolysis of H-hpp (**H-2**) under these conditions. The intermediate **20** could only be detected in traces, therefore methanolysis to **21** is considered to be somewhat faster than the initial intramolecular attack of the hydroxypropyl side chain to produce **20**.

Conclusion

Phosphate diesters are bound considerably more strongly by $Zr(TPP)(Cl)_2$ (**4**) than by the Zr^{IV}-complex **1**. Two main reasons are responsible for this: i) **1** offers only one complexation site for additional ligands to produce a charged 1:1 Zr:P complex whereas in **4** there are potentially four positions available (ligand exchange additionally provides charge neutral complexes); ii) phosphate diesters can be complexed in a dinuclear manner depending on the conditions. This was shown by ^{31}P-NMR spectroscopy, the X-ray analysis of the complex **19** and by kinetic analysis. The crystal structure of **19** reveals that dmp (**3**) is bound in a high energy *ap*,*ac* conformation and hydrolyzed if water is present. Comparison of P–O(ester) bonds indicates that electrostatic effects on bond lengths arising from metal complexation are much more important than stereoelectronic effects arising from conformational differences. Therefore phosphate diester activation for solvolysis is primarly achieved by Lewis acid activation, and the degree of activation is directly reflected in the P–O(ester) bond lengths with shorter bond distances indicating higher electrophilicity of the phosphorous atom. Note that this trend is opposite to that observed in ketal or acetal hydrolysis, where short C–O bond lengths indicate low reactivity.[41, 55]

$Zr(TPP)Cl_2$ (**4**) or its solvolysis products catalyse the solvolysis of the RNA-model phosphate hpp (**2**) as well as the DNA-model phosphate pmp (**16**). As determined by kinetic investigations, the active species in the solvolysis is a dinuclear Zr(TPP)-complex. The relative rate accelerations are comparable in magnitude to those of other dinuclear d-metal complexes and to those of the highly active mononuclear lanthanide complexes. The solvolysis of the DNA model pmp (**16**) by **4** is more accelerated than the transesterification of the RNA model hpp (**2**). $Zr(TPP)Cl_2$ (**4**) can thus be regarded as a precursor of a highly active catalyst for hydrolysis of DNA. The observation of two reaction pathways for transesterification of hpp (**2**) with different reaction order in phosphate is very unusual and has not been observed in transition metal catalysed transesterifications of **2** so far. The largest rate accelerations were measured in anhydrous solvents like C_6D_6/methanol and $CHCl_3$/methanol. In mildly acidic, water-containing solvents high initial rates could be observed, however, large turnover numbers were prevented by the formation of insoluble oxo- or hydroxo-complexes.

Further improvement of catalytic activity of such Zr^{IV}-TPP complexes seems to be possible by equipping the *meso*-phenyl substituents of TPP with catalytically competent general acid–base substituents or by linking two TPP units together, for example, via alkyne spacers,[56] to further promote binuclear complex formation.

Experimental Section

Materials and solvents: All reactions were performed under Schlenk-conditions using anhydrous solvents and flame-dried glassware unless otherwise stated. N_2 was flushed through a gas-washing bottle filled with activated BTS-catalyst (R 3–11, Fluka 18820) and molecular sieves (4 Å). Solvents were dried and distilled under N_2 prior to use: toluene (Na/benzophenone), chloroform (NaH), dichloromethane (NaH), methanol (Mg), pentane (NaH), 1,2,4-trichlorobenzene (molecular sieves 4 Å). Chemicals were used as purchased: $Zr(acac)_4$ (Fluka), phenol (Fluka), silicium tetrachloride ($SiCl_4$, Fluka), trimethyl chlorosilane (Me_3SiCl, Fluka), sodium acetate (Fluka, MolBio), acetic acid (Hänseler 99%). Chromatography was performed using redistilled solvents. Aluminium oxide was purchased from CAMAG (basic activity I). Ion-exchange resin (Amberlite IR-120 H^+ 16–45 mesh, Fluka was activated with 1N HCl for 24 h and washed with deionized water until neutral prior to use. 5,10,15,20-Tetraphenyl porphyrin (H_2tpp) was prepared according to the method of Lindsey and Wagner.[57] $ZrCl_4(2THF)$ was prepared according to the method of Manzer.[58]

Solvents used for the anhydrous kinetic measurements were distilled under N_2 (methanol from Mg, $CHCl_3$ from NaH) and filtered over basic alumina (CAMAG, activity I) prior to use. Deuterated solvents (ARMAR, ^{2}H-content $> 99.5\%$) were filtered over basic alumina. ^{1}H-NMR spectra were recorded at room temperature on a Bruker AC-300 (300 MHz) spectrometer. The solvents were used as internal standard, except in solvent mixtures where TMS was added as internal standard ($\delta = 0$). Complexation experiments and kinetics with ^{31}P-NMR spectroscopy were recorded on a Varian XL-200 (81 MHz) spectrometer equipped with a thermostat to maintain constant temperature during the experiment. ^{31}P-NMR control measurements for product distribution and the measurement of the dissociation constants were recorded on a Bruker AC-300 (121 MHz) spectrometer. Relaxation time for measurement of Zr^{IV}-phosphate complexes was raised from 0.5 to 1.5 s. Phosphorus chemical shifts are relative to H_3PO_4 as external standard. UV/Vis spectra were recorded on a Varian Cary 3E spectrophotometer equipped with a sample changer and a thermostat. MALDI-TOF-MS spectra were recorded on Linear Science Ltd. prototype (N_2-laser 337 nm, 0.28 μJ; pulse length 3 ns; extractor 11.0 kV; repeller 28.0 kV; detector -4.7 kV; positive mode) using 5,10,15,20-tetraphenyl porphyrin as matrix and internal standard ($M_r = 614.76$). All solutions were mixed using appropriate µL-syringes (Hamilton). The concentrations of the phosphate solutions correspond to phosphate concentration, not to salt concentration. hpp (**2**),[59] dmp (**3**)[60] and pmp (**16**)[61] were prepared according to literature procedures to give the phosphates as the following salts: $Ba(hpp)_2$, $Ba(pmp)_2$ and Na(dmp). These salts were used for the preparation of stock solutions.

$Zr(TPP)Cl_2$ (4): $SiCl_4$ (142 µL, 1.24 mmol) was added through a syringe to a solution of **5** (470 mg, 570 µmol) in toluene (7 mL) and the resulting deep-red mixture heated to reflux for 7 h (after 4 h additional 70 µL of $SiCl_4$ were added). The solution was cooled to room temperature and frozen with liquid nitrogen. The solvent was removed under reduced pressure and with consequent shaking of the flask to prevent bumping upon thawing of the mixture. The residue was dissolved in dichloromethane (10 mL), filtered through glass filter paper (Whatman) and transferred to a second flask using teflon tubes. The filtrate was concentrated to 5 mL, and after addition of 10 mL of pentane the solution was kept at $-20\,^{\circ}C$ overnight. The precipitated crystals were filtered off, washed with pentane (3×5 mL) and dried in vacuo to give **4** (397 mg, 90%) as deep-red needles. Analytical data matched those reported in the literature.[26]

$Zr(TPP)(OAc)_2$ (5): A mixture of H_2(TPP) (880 mg, 1.43 mmol), phenol (2.153 g, 22.9 mmol) and $Zr(acac)_4$ (1.396 g, 2.86 mmol) in trichlorobenzene (100 mL) was heated to 240 °C under Argon atmosphere using a sand

bath. After 24 hours the mixture was cooled to room temperature and the solvent removed under reduced pressure. The residue was dissolved in dichloromethane and applied onto an alumina column (4 × 11 cm). A violet fraction of unreacted H_2(TPP) was eluted with CH_2Cl_2, and a blood-red fraction of zirconium porphyrinates was collected with CH_2Cl_2/HOAc 30:2. The crude product was dissolved in pyridine/HOAc 4:6 (80 mL) and heated to reflux for 1 h. Water was added to the boiling solution, until the precipitation did no more dissolve (~10 mL), and the mixture was stored at 4 °C overnight. The crystals (pink needles) were collected on a glass fritted funnel, washed with water (3 × 10 mL) and dried in vacuo to yield Zr(TPP)$(OAc)_2 \cdot 0.6$ py (**5**) (1.153 g, 1.33 mmol, 93 %). Analytical data are identical to those reported in the literature.[24]

Zr(TPP)(OAc)Cl (6): Me_3SiCl (50 μL, 390 μmol) was added with a syringe to a solution of **5** (144 mg, 175 μmol) in toluene (5 mL). After the solution was stirred for 10 min, a red precipitate was observed. The mixture was heated to reflux for 7 h. The clear solution was cooled to room temperature, frozen with liquid N_2 and dried under high vacuum (careful watching for bumping while thawing is required). The residue was dissolved in CH_2Cl_2 (3 mL) and filtered through glass filter paper (Whatman) with teflon tubes. The filtrate was concentrated to ~1.5 mL, and after addition of 6 mL of pentane the solution was left to crystallise at −20 °C overnight. The crystals were filtered off, washed with pentane (2 × 3 mL) and dried in vacuo to yield **6** (128 mg, 160 μmol, 91 %) as blue-violet needles. ^{1}H NMR (300 MHz, $CDCl_3$): $\delta = 0.23$ (s, 3H; Zr-OAc), 7.79 (m, 12H; *m*,*p*-Ar-H), 8.08 (d, $J = 6.6$ Hz, 4H; *o*-Ar-Hα), 8.35 (br s, 4H; *o*-Ar-Hβ), 8.95 (s, 2H; β-H pyrrole), 9.05 (s, 6H; β-H pyrrole); ^{13}C NMR (75 MHz, $CDCl_3$): $\delta = 20.5$ (O_2C-*C*H_3), 125.3, 126.7, 127.9, 131.2, 133.1, 134.8, 142.2, 150.0; MALDI-TOF-MS: *m*/*z*: 798 $[M-1]^-$.

Zr(TPP)(OAc)(OMe) (8): Compound **4** (50 mg, 56 μmol) was dissolved in toluene (10 mL) and 18 μL $SiCl_4$ were added via syringe. The mixture was heated to reflux for three hours and then cooled to 80 °C. To the red solution potassium methanolate (4.0 mg, 565 μmol, freshly prepared from methanol and K) and methanol (10 μL) were added and the mixture stirred at 80 °C for three hours, cooled to room temperature and stirred for further 12 hours. After deep freezing the solution with liquid nitrogen the solvent was carefully removed under reduced pressure. The residue was dissolved in dichloromethane (10 mL), filtered through glass filter paper and transferred to a second flask via teflon capillary. The solvent was removed, and the resulting red powder vacuum dried to yield **8** (46 mg). According to ^{1}H-NMR spectroscopy the ratio of methoxide to acetate was 58:42. ^{1}H NMR (300 MHz, $CDCl_3/CD_3OD$ 1:1): $\delta = 0.28$ (br s, 3.48H; Zr-OAc), 1.28 (s, 2.52H; Zr-OMe), 7.81 (br s, 12H; *m*,*p*-Ar-H), 8.12 (s, 4H; *o*-Ar-H), 8.39 (s, 4H; *o*-Ar-H), 9.10 (s, 8H; β-H pyrrol).

Complexation of dmp (3) with 4, 5, 6 and 8: The following amounts of Zr^{IV}-porphyrinate were dissolved (700 μL $CDCl_3/CD_3OD$ 9:1 *v*/*v* each): solutions **A1**/**A2**/**A3**: 5.0 mg (6.45 μmol) **4** each, solution **B**: 4.7 mg (5.70 μmol) **5**, solution **C**: 5.0 mg (6.26 μmol) **6**, solution **D**: 5.0 mg (5.83 μmol) **8**. To the solutions were added the following amounts from a dmp(**3**) stock solution (250 mM in CD_3OD): **A1** +25 μL, **A2** +50 μL, **A3** +70 μL, **B** +60 μL, **C** +75 μL, **D** +30 μL. The solutions were well shaken in flame-sealed NMR tubes and examined with ^{1}H-NMR (300 MHz) and ^{31}P-NMR (81 MHz) spectroscopy during four days. The exact ratio of phosphate to zirconium porphyrinate was determined from the ^{1}H-NMR spectra. Ratio of the signals of free and complexed dmp (**3**) according to the ^{1}H-NMR and ^{31}P-NMR spectra (average of both) after four days (δ-values see text): **A1** 0:1, **A2** 1:1.22, **A3** 1:1.46, **B** 1:0, **C** 1:0.35, **D** 1:0.20.

Ligand exchange rate on 6 with dmp (3): To a solution of 5.0 mg of **6** (6.25 μmol, 500 μL $CDCl_3/CD_3OD$ 5:2 *v*/*v*) in a NMR tube was added 50 μL of a 125 mM dmp (**3**) solution (CD_3OD). Total volume: 550 μL, concentrations: [**6**] = [**3**] = 11.36 mM. The NMR tube was flame-sealed, well shaken ($t = 0$) and the complexation reaction followed by ^{1}H-NMR spectroscopy (300 MHz). The exchange rate constant was determined by using Equation (1) and the concentrations obtained from the ^{1}H-NMR spectra to yield a mean value of $k_2 = 3.6 \times 10^{-3}$ M^{-1}s^{-1} (Table 8).

$$k_2 \cdot t = \{1/([\text{dmp } (\mathbf{3})]_0 - [\text{Zr-dmp } (\mathbf{13})]_t)\} - (1/[\text{dmp } (\mathbf{3})]_0) \quad (1)$$

Ligand exchange rate on 4 with dmp (3): To a solution of 5.0 mg of **6** (6.44 μmol, 500 μL $CDCl_3/CD_3OD$ 5:2 *v*/*v*) in a NMR tube was added 103 μL of a 125 mM dmp (**3**) solution (CD_3OD). Total volume: 603 μL, concentrations: [**4**] = 10.68 mM, [**3**] = 21.36 mM. The NMR tube was flame-sealed, well shaken ($t = 0$) and the complexation reaction followed by ^{1}H-NMR spectroscopy (300 MHz). The exchange rate constant was determined from the slope of the exponential curve fit to the measured concentration of free dmp (**3**) (Table 9) versus time at $t = 0$ (Figure 2, $v_0 = 2.93 \times 10^{-5}$ M s^{-1}) using Equation (2):

$$v_0/([\text{Zr(TPP)Cl}_2\ (\mathbf{4})]_0 \cdot [\text{dmp } (\mathbf{3})]_0) = k_2 \quad (2)$$

Table 8.

t [s]	[dmp (**3**)] [mM]	[Zr-dmp] [mM]	k_2 [M^{-1}s^{-1}]
0	11.36	0	–
6000	9.10	2.26	3.644×10^{-3}
25200	5.69	5.67	3.481×10^{-3}
86400	2.53	8.83	3.556×10^{-3}

Table 9.

t [s]	[dmp (**3**)] [mM]
0	21.36
600	12.03
1200	10.27
1800	9.59
73800	8.24

Complexation of hpp (2) with 4, 6 and 8: The following amounts of Zr^{IV}-porphyrinate were dissolved (700 μL [D_6]DMSO/$CDCl_3$ 5:2 *v*/*v* each): solution **A**: 4.7 mg (5.70 μmol) of **5**, solution **B**: 5.0 mg (6.26 μmol) of **6**, solution **C**: 5.0 mg (6.45 μmol) of **4**, solution **D**: to solution **C** was added 50 μL of H_2O. To the solutions were added the following amounts from a hpp (**2**) stock solution (250 mM phosphate in [D_6]DMSO): **A** +6.8 μL, **B** +75 μL, **C** +77 μL, **D** +77 μL. The solutions were well shaken in flame-sealed NMR tubes and examined with ^{1}H-NMR and ^{31}P-NMR spectroscopy. Solutions **A** and **B** showed no evidence of complexed hpp (**2**). ^{1}H-NMR (300 MHz) and relative integrals (only CH_3 signals of hpp (**2**) are given) of solution **C**: $\delta = 0.98$ (0.57), 0.76 (0.21), 0.52 (0.22); ^{31}P-NMR (81 MHz) and relative integrals: solution **C**: −4 (0.57), −16 (0.29), −18 (0.14); solution **D**: −6 (0.44), −14/−17 (0.35), −24 (0.21). Measurement of solution **D** required ~20 000 scans.

Experiments for the determination of dissociation constants: Stock solutions: **A**: 20 mM of **4** (C_6D_6) +20 μL per mL of 1N NaOMe (MeOH); **B**: 80 mM **3** (MeOH). Two equivalents of NaOMe were added to **4** to avoid liberation of HCl due to ligand exchange of chloride with methanol; solution **A** was stable for 24 h at room temperature before precipitation occurred. For the measurement the following mixtures were prepared: **a**: 125 μL **A** +250 μL **B**; **b**: 50 μL **A** +31 μL **B**; **c**: 250 μL **A** +6.25 μL **B**. Solutions **a** to **c** were prepared in a NMR tube and methanol and C_6D_6 was added to give a final volume of 500 μL with C_6D_6/methanol 1:1 *v*/*v*. Each sample was measured with ^{31}P-NMR spectroscopy (~30 000 scans). The dissociation constants were calculated for the equilibrium

$$\text{Zr(TPP)Cl}_2\ (\mathbf{4}) + \text{dmp } (\mathbf{3}) \rightleftharpoons ([\text{Zr(TPP)(dmp),(X)}])$$

using Equation (3):

$$K_D = [\mathbf{4}] \cdot [\text{dmp } (\mathbf{3})]/(\Sigma[\text{Zr(TPP)(dmp)(X)}]) \quad (3)$$

The concentration in the samples were as follows: **a**: [**4**] = 5 mM, [**3**] = 40 mM; **b**: [**4**] = 2 mM, [**3**] = 5 mM; **c**: [**4**] = 10 mM, [**3**] = 1 mM. ^{31}P NMR (121 MHz) with relative integrals: **a**: $\delta = 5$ (0.89), −3 (0.11); **b**: $\delta = 5$ (0.69), −3 (0.21), −16 (0.10); **c**: $\delta = 5$ (0.07), −16 (0.93).

(μ-η^2-mmp)(μ-dmp)$_2$[Zr(TPP)]$_2$ (19): To 30 mg (38.6 μmol) Zr(TPP)Cl_2 **4** in anhydrous $CHCl_3$ (10 mL) under Ar atmosphere were added 400 μL of a dmp (**3**) solution (250 mM in anhydrous methanol), and the resulting mixture was stirred at room temperature for three days. The solvent was evaporated, and the red powder was dissolved in anhydrous toluene and filtered through a glass fritted funnel to remove inorganic salts. The filtrate was evaporated to dryness to give a red crystalline powder (36 mg). ^{1}H NMR (300 MHz, $CDCl_3$): $\delta = 8.64$ (s, 2H), 8.62 (s, 2H), 8.57 (s, 2H), 8.55 (s, 2H), 8.20 (m, 2H), 7.51–7.77 (m, 18H), 1.52 (d, $J = 11.7$ Hz, 2.5H), 1.44

0947-6539/00/0603-0534 $ 17.50+.50/0 *Chem. Eur. J.* **2000**, *6*, No. 3

(dd, $J = 3.7$, 11.7 Hz, 2.1 H), 1.23 (s, 5H, Zr-OCH_3), 1.13 (d, $J = 11.7$ Hz, 2.3 H); ^{31}P-NMR (81 MHz, $CDCl_3$): $\delta = -8$, -13, -14, -19; MALDI-TOF-MS: $m/z = 1464$, 1347, 851, 789, 762, 718.

The crystalline residue (10 mg) was dissolved in anhydrous toluene (2 mL) and stored at $-20\,^{\circ}$C. Every four days anhydrous pentane (10 μL) was added to the blood-red solution, and after one and a half months red, cubic crystals were grown suitable for X-ray analysis. ^{31}P NMR (121 MHz, $CDCl_3$): $\delta = -12$ (s, 0.1), -16 (s, 0.7), -19 (s, 0.2); MALDI-TOF-MS: $m/z = 1695$, 1645, 831, 743.

X-ray structure determination: Data were collected on a Siemens Smart CCD at 200 K. The structure was solved by direct methods and refined by using the SHELX-97 program. The refinement was carried out by full-matrix least-squares procedures on F^2. Hydrogen atoms were refined isotropically using a riding model. The asymmetric unit contains one toluene molecule distributed over two positions. Crystal data: $C_{57}H_{47}N_4O_6P_{1.5}Zr_1$, $M_r = 1022.22$ (asymmetric unit), colour blood-red, shape rhombic, $0.07 \times 0.09 \times 0.18$ mm, triclinic, $P1$, $a = 12.546(3)$ Å, $b = 12.964(3)$ Å, $c = 15.741(3)$ Å, $\alpha = 73.39(3)^{\circ}$, $\beta = 83.33(3)^{\circ}$, $\gamma = 83.00(3)^{\circ}$, $V = 2426.2(8)$ Å^3, $Z = 2$, $\rho = 1.398$ g cm^{-3}, $\mu = 0.333$ mm^{-1}, $F(000) = 1055$, radiation $Mo_{K\alpha}$, $\lambda = 0.71073$ Å, θ_{max} 26.78°, $-15 < h < 14$, $-15 < k < 14$, $-17 < l < 19$, 12443 total measured data, 8877 unique data, 5929 observed data with $I > 2\sigma(I)$, $R_{int} = 0.0534$, $R = 0.0950$, 713 parameters, 233 restraints, R_1 (for $F > 2(F)$) $= 0.0891$, R_1 (all data $= 0.1584$, $wR2$ (all data $= 0.1657$, $S = 1.205$ (restrained 1.189), max./min. difference peak 1.084/-1.003 e Å^3. Crystallographic data (excluding structure factors) have been deposited with the Cambridge Crystallographic Data Centre as supplementary publication no. CCDC-133297. Copies of the data can be obtained free of charge on application to CCDC, 12 Union Road, Cambridge CB2 1EZ, UK (fax: (+44) 1223-336-033; e-mail: deposit@ccdc.cam.ac.uk).

Reesterification of 2 with 4 in C_6D_6/methanol 1:1: The following stock solutions were prepared: **A**: 10 mM **4** (C_6D_6) +20 μL per mL 1N NaOMe (MeOH); **B**: 80 mM **2** (MeOH). Addition of 2 equiv of NaOMe to **4** was done to avoid liberation of HCl due to ligand exchange of chloride with methanol; solution **A** was stable for 24 h at room temperature before precipitation occurred. For kinetic measurement appropriate amounts of solns. **A** and **B** were mixed in NMR tubes and complemented with C_6D_6 and methanol to give a final volume of 500 μL (C_6D_6/methanol 1:1) to give the following concentrations of **4** and **2** in the mixtures (mM): 2+8, 2+12, 2+20, 2+28, 2+32, 2+40, 1.5+32, 3+32, 4+32, 4.5+32, 5+32. The NMR tubes were flame-sealed, well shaken ($t = 0$) and the reaction was monitored by ^{31}P-NMR spectroscopy at $T = 28\,^{\circ}$C. The rate constants were obtained by fitting the concentrations with curves according to the equations used for a consecutive irreversible pseudo first order reaction.[47]; The reaction orders were obtained from a double logarithmic plot of the initial rates v_0 of the depletion of **2** (obtained from the slope of the fitted exponential curve to the measured concentration of **2** versus time at $t = 0$) versus concentration.

Saturation kinetics of the reaction of 2 and 16 with 4 in $CHCl_3$/methanol 1:4 in the presence of imidazole: 1) General procedure for the preparation of the reaction mixtures and measurement. The following stock solutions were prepared: **A**: 1.11 mM **4** (8.60 mg per 10 mL $CHCl_3$/methanol 1:4), **B**: 50 mM **2** (methanol), **C**: 50 mM **16** (methanol), **D**: 1.0 M imidazole (methanol), **E**: 100 mM tris/HCl pH 9.0 +10 mM NaOAc (H_2O). The reaction mixtures were prepared from solutions **A**, **B**, **C** and **D** so that [**4**] = 1.0 mM, [imidazole] = 20.0 mM and [**2**] or [**16**] = 0.25, 0.5, 0.75, 1.0, 2.0 or 4.0 mM resulted in a total sample volume of 1.0 mL. The mixtures were prepared in Eppendorf tubes, well shaken and placed in a thermostate at $T = 30\,^{\circ}$C. Aliquots of the reaction mixtures were withdrawn and mixed with solution **E** to stop the reaction and to get a maximum possible phenolate concentration of 0.1 to 0.8 mM in the aqueous phase (100 to 200 μL reaction mixture + 300 to 900 μL solution **E**). The suspensions obtained this way were centrifuged (2 min. at 5000 rpm), and UV/Vis spectra were recorded from the aqueous phases. From the spectra the first derivatives were calculated, and the percentage of released phenolate was calculated from the ratios of the peak intensities at 258 nm to 270 nm and 270 nm to 278 nm according to Equations (4) and (5) (A = absorption, x = percentage of hydrolysed phosphate, $r1 = A(258\text{ nm})/A(270\text{ nm})$, $r2 = A(270\text{ nm})/A(278\text{ nm})$):

$$x1 = -30.14 + 100.62 \cdot r1 \quad (4)$$

$$x2 = -1.943 + 27.94 \cdot \exp(-(r2 - 0.293)/3.687) + 68.48 \cdot \exp(-(r2 - 0.293)/0.473) \quad (5)$$

The final concentration of phenolate was calculated from the mean value of x1 and x2 and the corresponding initial concentrations of phosphates. The Michaelis–Menten parameters were obtained from the initial rates v_0 of the reactions according to the usual equations used for saturation kinetics.[47] All reactions were performed in triple runs. The background reactions were similarly measured in the absence of **4**.

Reesterification of H-2 with 4 in [D_6]DMSO/$CHCl_3$/H_2O 5:5:1: To 5.0 mg of **4** (6.45 μmol in 550 μL [D_6]DMSO/$CHCl_3$/H_2O 5:5:1) was added in a NMR tube 262 μL of a **H-2** solution (34.3 mg in 2.0 mL $CHCl_3$). The NMR tube was flame-sealed, well shaken and the progress of the reaction was monitored with ^{31}P-NMR spectroscopy at room temperature. The pseudo first order reaction rate was obtained from the usual procedure used for a first order reaction using Equation (6):

$$\ln([\mathbf{H\text{-}2}]_t/[\mathbf{H\text{-}2}]_0) = -k \cdot t \quad (6)$$

The background reaction was similarly measured in the absence of **4**.

Reesterification of 2 with 4 in C_6D_6/methanol/H_2O 5:5:1, pH 6.0: The following solutions were prepared: **A**: 9.78 mM **4** (C_6D_6), **B**: 80 mM **2** (methanol), **C**: 1.0 M imidazole/HCl pH 6.0 (H_2O). Reaction mixture: in a NMR tube 100 μL of solution **A**, 100 μL of solution **B** and 60 μL of solution **C** were added to 400 μL C_6D_6/methanol 1:1. The NMR tube was flame-sealed, well shaken and the reaction followed by ^{31}P-NMR spectroscopy at $T = 40\,^{\circ}$C. The initial rate v_0 was obtained from the slope of the exponential curve fit to the measured concentration of **2** versus time at $t = 0$.

Acknowledgment

Financial support from the Swiss National Science Foundation, as well as a grant to E.S. from the "Stipendienfonds der Basler Chemischen Industrie zur Unterstützung von Doktoranden auf dem Gebiete der Chemie der Biotechnologie und der Pharmazie" is gratefully acknowledged. We thank Prof. P. Bigler und PD Dr. T. Ward for help with NMR experiments, B. Therrien for help with X-ray experiments, and H. Trafelet and Dr. S. Schuerch for measurement of the MALDI-TOF-MS spectra.

[1] a) E. Kövári, R. Krämer, *J. Am. Chem. Soc.* **1996**, *118*, 12704–12709; b) J. Chin, *Acc. Chem. Res.* **1991**, *24*, 145–152; c) D. Magda, R. A. Miller, J. L. Sessler, *J. Am. Chem. Soc.* **1994**, *116*, 7439–7440; d) J. R. Lorsch, J. W. Szostak, *Acc. Chem. Res.* **1996**, *29*, 103–110.

[2] a) J. H. Kim, J. Chin, *J. Am. Chem. Soc.* **1992**, *114*, 9792–9795; b) J. Suh, N. Kim, H. S. Cho, *Bioorg. Med. Chem. Lett.* **1994**, *4*, 1889–1892; c) M. Yashiro, A. Ishikubo, M. Komiyama, *J. Chem. Soc. Chem. Commun.* **1995**, 1793–1794; d) K. G. Ragunathan, H.-J. Schneider, *Angew. Chem.* **1996**, *108*, 1314–1316; *Angew. Chem. Intl. Ed. Engl.* **1996**, *35*, 1219–1221 e) N. H. Williams, J. Chin, *Chem. Commun.* **1996**, 131–132; f) N. Sträter, W. N. Lipscomb, T. Klabunde, B. Krebs, *Angew. Chem.* **1996**, *108*, 2158–2190; *Angew. Chem. Int. Ed. Engl.* **1996**, *35*, 2024–2055; g) M. Komiyama, Y. Matsumoto, H. Zakahashi, T. Shiiba, H. Tsuzuki, H, Yajima, M. Yashiro, J. Sumaoka, *J. Chem. Soc. Perkin Trans. 2* **1998**, 691–695.

[3] a) J. R. Morrow, L. A. Buttrey, V. M. Shelton, K. A. Berback, *J. Am. Chem. Soc.* **1992**, *114*, 1903–1905; b) Y. Matsumoto, M. Komiyama, *Nucleic Acid Symp. Ser.* **1992**, *27*, 33–34; c) J. Sumaoka, S. Miyama, M. Komiyama, *Chem. Commun.* **1994**, 1755–1756; d) R. A. Moss, B. D. Park, P. Scrimin, G. Ghirlanda, *Chem. Commun.* **1995**, 1627–1628; e) J. Rammo, R. Hettich, A. Roigk, H.-J. Schneider, *Chem. Commun.* **1996**, 105–107; f) J. Sumaoka, Y. Azuma, M. Komiyama, *Chem. Eur. J.* **1998**, *4*, 205–209; g) J. Kamitani, J. Sumaoka, H. Asanuma, M. Komiyami, *J. Chem. Soc. Perkin Trans. 2* **1998**, 523–527.

[4] a) R. Breslow, E. Anslyn, D.-L. Huang, *Tetrahedron* **1991**, *47*, 2365–2376; b) R. Gross, G. Dürner, M. W. Göbel, *Liebigs Ann. Chem.* **1994**, 49–58; c) M.-S. Muche, M. W. Göbel, *Angew. Chem.* **1996**, *108*, 2263–2265; *Angew. Chem. Int. Ed. Engl.* **1996**, *35*, 2126–2129; d) T. Kato, T.

Takeuchi, I. Karube, *Chem. Commun.* **1996**, 953 – 954; e) V. Jubian, A. Veronese, R. P. Dixon, A. D. Hamilton, *Angew. Chem.* **1995**, *107*, 1343 – 1345; *Angew. Chem. Int. Ed. Engl.* **1995**, *34*, 1237 – 1239.
[5] a) R. Häner, J. Hall, G. Ryhs, *Helv. Chim. Acta* **1997**, *80*, 487 – 494; b) M. P. Fitzsimons, J. K. Barton, *J. Am. Chem. Soc.* **1997**, *119*, 3379 – 3380; c) K. Michaelis, M. Kalesse, *Angew. Chem.* **1999**, *111*, 2382 – 2385; *Angew. Chem. Int. Ed.* **1999**, *38*, 2243 – 2245; d) M. Komiyama, T. Inokawa, K. Yoshinari, *Chem. Commun.* **1995**, 77 – 78.
[6] B. D. Wladkowski, L. A. Svensson, L. Sjolin, J. E. Ladner, G. L. Gilliland, *J. Am. Chem. Soc.* **1998**, *120*, 5488 – 5498.
[7] U. Heinemann, W. Saenger, *Nature* **1983**, *299*, 27 – 31.
[8] D. Suck, C. Oefner, *Nature* **1986**, *321*, 620 – 625.
[9] a) W. B. Knight, S. W. Fitts, D. Dunawaya-Mariano, *Biochem.* **1981**, *20*, 4079 – 4086; b) G. P. Haight, *Coord. Chem. Rev.* **1987**, *79*, 293 – 319.
[10] F. A. Cotton, E. E. Hazen, M. J. Legg, *Proc. Natl. Acad. Sci. USA* **1979**, *76*, 2551 – 2555.
[11] I. Bertini, C. Luchinat, W. Maret, M. Zeppezauer, *Zinc Enzymes*, Birkhäuser, **1986**.
[12] J. Smith, K. Ariga, E. V. Anslyn, *J. Am. Chem. Soc.* **1993**, *115*, 362 – 364.
[13] J. R. Morrow, W. C. Trogler, *Inorg. Chem.* **1988**, *27*, 3387 – 3394.
[14] a) D. S. Sigman, A. Mazumber, D. M. Perrin, *Chem. Rev.* **1993**, *93*, 2295 – 2316; b) J. Chin, M. Banaszczyk, V. Jubian, X. Zou, *J. Am. Chem. Soc.* **1989**, *111*, 186 – 190; c) C. Kurz, *Chem. uns. Zeit* **1998**, *32*, 94 – 103.
[15] a) R. Breslow, D. Berger, D.-L. Huang, *J. Am. Chem. Soc.* **1990**, *112*, 3686 – 3687; b) J. R. Morrow, H. Aures, D. Epstein, *Chem. Commun.* **1995**, 2431 – 2432; c) J. Suh, J. Y. Lee, S. H. Hong, *Bioorg. Med. Chem. Lett.* **1997**, *7*, 2383 – 2386.
[16] a) I. Török, T. Gajda, B. Gyurcsik, G. K. Tóth, A. Péter, *J. Chem. Soc. Dalton Trans.* **1998**, 1205 – 1212; b) F. Chu, J. Smith, V. M. Lynch, E. V. Anslyn, *Inorg. Chem.* **1995**, *34*, 5689 – 5690.
[17] J. W. Buchler, in *Porphyrins and Metalloporphyrins* (Ed.: K. M. Smith), Elsevier, **1975**, p. 157.
[18] In order for a complex of a nonessential metal to function in vivo it is necessary that the complex is inert to release of the metal ion. See [1a][3a].
[19] a) J. L. Hoard, in *Porphyrins and Metalloporphyrins* (Ed.: K. M. Smith), Elsevier, **1975**, p. 347; b) W. R. Scheidt, in *The Porphyrins, Physical Chemistry Part A* (Ed.: D. Dolphin), Academic Press, **1978**, p. 463; c) J. L. Huhmann, J. Y. Corey, N. P. Rath, *Acta Crystallogr. Sect. C* **1995**, 195 – 196.
[20] E. Bamann, *Angew. Chem.* **1939**, *52*, 186 – 188.
[21] After the work of Bamann[20] only three reports (besides[22]) concerned with the use of Zr^{4+}-salts in phosphate diester hydrolysis seem to have appeared: a) R. A. Moss, J. Zhang, K. G. Rangunathan, *Tetrahedron Lett.* **1998**, *39*, 1529 – 1532; b) R. Ott, R. Krämer, *Angew. Chem.* **1998**, *110*, 2064 – 2067; *Angew. Chem. Intl. Ed.* **1998**, *37*, 1957 – 1960; c) A. Berkessel, D. A. Hérault, *Angew. Chem.* **1999**, *111*, 99 – 102; *Angew. Chem. Intl. Ed.* **1999**, *38*, 102 – 105.
[22] E. Stulz, C. Leumann, *Chem. Commun.* **1999**, *3*, 239 – 240.
[23] J. W. Buchler, G. Eikelmann, L. Puppe, K. Rohbock, H. H. Schneehage, D. Weck, *Liebigs Ann. Chem.* **1971**, *745*, 135 – 151.
[24] K. Shibata, T. Aida, S. Inoue, *Tetrahedron Lett.* **1992**, *33*, 1077 – 1080.
[25] H. Brand, J. Arnold, *Organometallics* **1993**, *12*, 3655 – 3665.
[26] H.-J. Kim, D. Whang, K. Kim, Y. Do, *Inorg. Chem.* **1993**, *32*, 360 – 362.
[27] J. K. M. Sanders, B. K. Hunter, in *Modern NMR Spectroscopy: A Guide for Chemists*, 2nd Ed., Oxford University Press, Oxford, **1993**, chapter 7.
[28] T. R. Janson, J. J. Katz in *The Porphyrins, Physical Chemistry Part A* (Ed.: D. Dolphin), Academic Press **1978**, p. 1.
[29] D. Wahnon, A.-M. Lebuis, J. Chin, *Angew. Chem.* **1995**, *107*, 2594 – 2597; *Angew. Chem. Intl. Ed.* **1995**, *34*, 2412 – 2414.
[30] a) H.-J. Kim, D. Wang, Y. Do, *Chem. Lett.* **1993**, 807 – 810; b) J. L. Huhmann, J. Y. Corey, N. P. Rath, C. F. Campana, *J. Organomet. Chem.* **1996**, *513*, 17 – 26.
[31] H. Brand, J. Arnold, *J. Am. Chem. Soc.* **1992**, *114*, 2266 – 2267.
[32] W. Saenger, in *Principles of Nucleic Acids Structure*, Springer, **1984**, chapter 4.
[33] B. Schneider, M. Kabelaž, P. Hobza, *J. Am. Chem. Soc.* **1996**, *118*, 12207 – 12217.
[34] D. G. Gorenstein, in *Phosphorus-31 NMR, Principles and Applications*, Academic Press, N.Y. **1984**, chapter 1.
[35] a) D. G. Gorenstein, B. Findlay, B. A. Luxon, D. Kar, *J. Am. Chem. Soc.* **1977**, *99*, 3473 – 3479; b) D. G. Gorenstein, D. Kar, *J. Am. Chem. Soc.* **1977**, *99*, 672 – 677.
[36] The values for the P–O(ester) bond lengths range from 1.547 Å to 1.631 Å, for the P=O bond lengths from 1.433 Å to 1.590 Å.
[37] D. W. Cruickshank, *J. Chem. Soc.* **1961**, 5486 – 5504.
[38] J. P. Hazel, R. L. Collin, *Acta Crystallogr. Sect. B* **1972**, *28*, 2951 – 2957.
[39] W. T.A Harrison, T. M. Nenoff, T. E. Gier, G. D. Stucky, *J. Mater. Chem.* **1994**, *4*, 1111 – 1115.
[40] D. F. Shriver, P. W. Atkins, C. H. Langford, in *Inorganic Chemistry*, 1st Ed., Oxford University Press, **1990**.
[41] A. J. Kirby, The Anomeric Effect and Related Stereoelectronic Effects at Oxygen in *Reactivity and Structure Concepts in Organic Chemistry*, *Vol. 15*, Springer, N.Y., **1983**.
[42] a) D. G. Gorenstein, A. Chang, J.-C. Yang, *Tetrahedron* **1987**, *43*, 469 – 478; b) R. Kluger, G. R. J. Thatcher, *J. Org. Chem.* **1986**, *51*, 207 – 212; c) R. Kluger, G. R. J. Thatcher, *J. Am. Chem. Soc.* **1985**, *107*, 6006 – 6011; d) K. Taira, T. Fanni, D. G. Gorenstein, *J. Org. Chem.* **1984**, *49*, 4531 – 4536.
[43] N.-Y. Chang, C. Lim, *J. Am. Chem. Soc.* **1998**, *120*, 2156 – 2167, and references therein.
[44] J. R. Morrow, W. C. Trogler, *Inorg. Chem.* **1988**, *27*, 3387 – 3394.
[45] B. K. Takasaki, J. Chin, *J. Am. Chem. Soc.* **1994**, *116*, 1121 – 1122.
[46] J. Sumaoka, Y. Azuma, M. Komiyama, *Chem. Eur. J.* **1998**, *4*, 205 – 209.
[47] A. Fersht, in *Enzyme Structure and Mechanism*, 2nd Ed., Freeman, N.Y., **1985**.
[48] Inspection of the dissociation constants obtained by complexation experiments and saturation kinetics revealed that the difference in phosphate complex stability is only slightly dependent upon the nature of the phosphate. Generally dmp (**3**) and pmp (**16**) are somewhat less strongly complexed than hpp (**2**). The average K_d (phosphate) for a dinuclear zirconium complex from all values determined here is $K_d = 0.5(1)$ mM.
[49] The second order rate constants for the background reactions were measured at [NaOMe] = 1 mM to be $k_{2,0} = 2.93 \times 10^{-3}\,M^{-1}s^{-1}$ (**2** → **20**), $1.97 \times 10^{-3}\,M^{-1}s^{-1}$ (**20** → **21**) and at [NaOMe] = 100 mM $3.11 \times 10^{-6}\,M^{-1}s^{-1}$ (**16** → **3**). The pH of C_6D_6/methanol 1:1 was 8.2 corresponding to $[MeO^-] = 6.3 \times 10^{-9}$ M and did not change during the catalytic and background reactions. With $k_{1,0} = k_{2,0} \times [MeO^-]$ the first order background rate constants were extrapolated to the conditions used in the catalysed reactions.
[50] Reactions proceeding predominantly according to pathway b) could only be measured at [**4**] = 2 mM and [**2**] = 8 mM. The apparent second order rate constant was obtained from $k_2 = k_1/[\mathbf{4}]$.
[51] R. A. Moss, J. Zhang, K. Bracken, *Chem. Commun.* **1997**, 1639 – 1640.
[52] In neutral water-containing solvents no solvolysis of **2** with **4** was observed. Addition of bases (NaOH, NEt_3 or imidazole) resulted in rapid and complete precipitation of the Zr(TPP) complexes.
[53] The background reaction rate for the transesterification of H-hpp (**H-2**) ([D_6]DMSO/$CHCl_3$/H_2O 5:5:1, [H^+] = [H-hpp (**H-2**)] = 23.8 mM) was measured to be $k_{1,0} = 3.21 \times 10^{-7}\,s^{-1}$. From this, the value for the background reaction in C_6D_6/methanol/H_2O 5:5:1 (pH 6.0) was calculated to be $k_{1,0} = 1.35 \times 10^{-11}\,s^{-1}$ without correction for the different solvents.
[54] For the determination of total H^+-concentration it is assumed that $Zr(TPP)Cl_2$ (**4**) reacts rapidly with water to produce hydroxo-complexes with liberation of two equivalents of HCl, which serve as an additional source of protons together with **H-2** (predominantly being in the dissociated form).
[55] H. B. Bürgi, K. C. Steudle, *J. Am. Chem. Soc.* **1988**, *110*, 7291 – 7299.
[56] V. Marvaud, A. Vidal-Ferran, S. J. Webb, J. K. M. Sanders, *J. Chem. Soc. Dalton Trans.* **1997**, 985 – 990.
[57] J. S. Lindsey, R. W. Wagner, *J. Org. Chem.* **1989**, *54*, 828.
[58] L. E. Manzer, *Inorg. Synth.* **1982**, *21*, 135.
[59] D. M. Brown, D. A. Usher, *J. Chem. Soc.* **1965**, 6558 – 6564.
[60] R. A. McIvor, G. D. McCarthy, G. A. Grant, *Can. J. Chem.* **1956**, *34*, 1819 – 1832.
[61] R. J. P. Corriu, G. F. Lanneau, D. Leclerq, *Tetrahedron* **1986**, *42*, 5591 – 5600.

Received: August 12, 1999 [F1973]

  0947-6539/00/0603-0536 $ 17.50+.50/0 *Chem. Eur. J.* **2000**, *6*, No. 3